

Journal: ACP

Title: Molecular characteristics and diurnal variations of organic aerosols at a rural site in the North China Plain with implications for the influence of regional biomass burning

Author(s): Jianjun Li et al.

MS No.: acp-2019-75

Dear Editor,

We thank you very much for the comments. In this manuscript, we checked the text for grammar mistakes carefully. Please see the details in the following marked-up manuscript.

Anything about our paper, please feel free to contact me at ghwang@geo.ecnu.edu.cn.

Best regards,

Sincerely yours

Gehui Wang

Jul. 28, 2019

1 **Molecular characteristics and diurnal variations of organic aerosols**
2 **at a rural site in the North China Plain with implications for the**
3 **influence of regional biomass burning**
4
5

6 Jianjun Li^{1,4}, Gehui Wang^{1,2,3*}, Qi Zhang^{4*}, Jin Li¹, Can Wu², Wenqing Jiang⁴, Tong
7 Zhu⁵, and Limin Zeng⁵
8
9

10 ¹Key Lab of Aerosol Chemistry & Physics, SKLLQG, Institute of Earth Environment,
11 Chinese Academy of Sciences, Xi'an 710061, China

12 ²Key Laboratory of Geographic Information Science of the Ministry of Education,
13 School of Geographic Sciences, East China Normal University, Shanghai 200241,
14 China

15 ³Institute of Eco-Chongming, 3663 N. Zhongshan Rd., Shanghai 200062, China

16 ⁴Department of Environmental Toxicology, University of California, Davis, CA
17 95616, USA

18 ⁵BIC-ESAT and SKL-ESPC, College of Environmental Sciences and Engineering,
19 Peking University, Beijing, China
20
21
22
23

24 *Corresponding authors:

25 Prof. Gehui Wang, E-mail: ghwang@geo.ecnu.edu.cn;

26 Prof. Qi Zhang, E-mail: dkwzhang@ucdavis.edu
27
28

29 **Abstract**

30 Field burning of crop residue in early summer releases into the atmosphere a
31 large amount of pollutants with significant impacts on the air quality and aerosol
32 properties in the North China Plain (NCP). In order to investigate the influence of this
33 regional anthropogenic activity on molecular characteristics of organic aerosols, ~~we~~
34 ~~collected~~ PM_{2.5} filter samples ~~every were collected with a 3-hours~~ 3-hr interval at a
35 rural site of NCP ~~during from~~ June 10th to 25th, 2013, and analyzed ~~them~~ for more
36 than 100 organic tracer compounds, including both primary (*n*-alkanes, fatty
37 acids/alcohols, sugar compounds, polycyclic aromatic hydrocarbons, hopanes, and
38 phthalate esters) and secondary (~~phthalic acids, isoprene, α - β pinene, β -~~
39 ~~caryophyllene, and toluene-derived products~~) organic aerosol (SOA) tracers (phthalic
40 acids, isoprene-, α - β -pinene, β -caryophyllene, and toluene-derived products), ~~as~~
41 well as ~~for~~ organic carbon (OC), elemental carbon (EC), and water-soluble organic
42 carbon (WSOC). Total concentrations of the measured organics ranged from 177 to
43 6248 ng m⁻³ (mean 1806 \pm 1308 ng m⁻³) during the study period, most of which were
44 contributed by sugar compounds, followed by fatty acids and fatty alcohols.
45 Levoglucosan (240 \pm 288 ng m⁻³) was the most abundant single compound and
46 strongly correlated with OC and WSOC, suggesting that biomass burning (BB) is an
47 important source of summertime organic aerosols in this rural region. Based on the
48 analysis of fire spots and backward trajectories of air masses, two representative
49 periods were classified, which are (1) Period 1 (P1), Jun 13th 21:00-16th 15:00, when
50 air masses were uniformly from the southeast part of NCP, where intensive open-field
51 ~~biomass burning~~ biomass burning (BB) occurred; and (2) Period 2 (P2), Jun 22nd

52 12:00-24th 06:00, which is representative of local emission. Nearly all the measured
53 PM components showed much higher concentrations in P1 than in P2. Although *n*-
54 alkanes, fatty acids, and fatty alcohols presented similar temporal/diurnal variations as
55 those of levoglucosan throughout the entire period, their molecular distributions were
56 more dominated by high molecular weight (HMW) compounds in P1, demonstrating
57 an enhanced contribution from BB emissions. In contrast, intensive BB emission in
58 P1 seems to have limited influences on the concentrations of polycyclic aromatic
59 hydrocarbons (PAHs), hopanes and phthalate esters. Both 3-hydroxyglutaric acid and
60 β -caryophyllinic acid showed strong linearly correlations with levoglucosan ($R^2=0.72$
61 and 0.80, respectively), indicating that BB is also an important source for terpene-
62 derived SOA formation. A tracer-based method was used to estimate the distributions
63 of biomass-burning OC, fungal-spore OC and secondary organic carbon (SOC)
64 derived from isoprene, α -/ β -pinene, β -caryophyllene, and toluene in the different
65 periods. The results showed that the contribution of biomass-burning OC to total OC
66 in P1 (27.6%) was 1.7 times of that in P2 (17.1%). However, the contribution of SOC
67 from oxidation of the four kinds of [volatile organic compounds \(VOCs\)](#) increased
68 slightly from 16.3% in P1 to 21.1% in P2.

69 **Key words:** Organic aerosols; Molecular composition; North China Plain; Biomass
70 Burning

71

72 1. Introduction

73 Organic aerosols (OA, i.e., the organic fraction of particles) constitute a substantial
74 fraction (~10-90%) (~~Jimenez et al., 2009; Zhang et al., 2007a; Hallquist et al., 2009~~) of
75 atmospheric particles (Jimenez et al., 2009; Zhang et al., 2007a; Hallquist et al., 2009),
76 and have significant effects on global and regional climate (Venkataraman et al.,
77 2005; Kanakidou et al., 2005), air quality (Aggarwal et al., 2013; Wang et al., 2006b),
78 human health (Lelieveld et al., 2015), and ecosystems (Tie et al., 2016). Organic
79 aerosols in the atmosphere can be emitted directly from various sources, such as
80 ~~combustion of~~ fossil fuels combustion, biomass burning, plant emission, and so on,
81 which is defined as primary organic aerosols (POA). On the other hand, atmospheric
82 secondary OA (SOA) are produced from photochemical oxidation products of volatile
83 organic compounds (VOCs) via gas-particle conversion processes such as nucleation,
84 condensation and heterogeneous chemical reactions (Hallquist et al., 2009). These
85 organic species could modify physicochemical characteristics of atmospheric aerosols
86 such as hygroscopicity, albedo, and oxidation state (Dinar et al., 2008; Chan et al.,
87 2005; Fu et al., 2010). Thus, a thorough understanding of molecular composition and
88 source of organic aerosols is necessary in order to address aerosol related environmental
89 issues and to improve the accuracy of modelling studies.

90 Tremendous amounts of air pollutants including both particulate matters (PM) and
91 their gaseous precursors (e.g., SO₂, NO_x, NH₃, and VOCs) are emitted into the
92 atmosphere from power plants, industries and vehicles due to rapid economy
93 development in China, leading to serious air ~~conditions-pollution~~ in the recent decades

域代码已更改

域代码已更改

94 (Zhang et al., 2009;Guo et al., 2014;Wang et al., 2016;Huang et al., 2014;Li et al., 2017).
95 The North China Plain (NCP) has been recognized as one of the most polluted regions
96 in the world, with very high concentrations of PM_{2.5} on the ground surface (van
97 Donkelaar et al., 2010). The NCP is also one of the most significant aerosol sources in
98 the world, which has a significant impact on the East China Sea and Western North
99 Pacific (Andreae and Rosenfeld, 2008). Thus, extensive efforts have been made in
100 recent years to characterize the sources, properties, and processes of PM in the NCP.
101 Most of these results concluded that the severe air pollution in the region is related to
102 the source strength and frequently happens under stagnant weather conditions. Recently,
103 ~~it has been studies shown~~ showed that the rapid growth of secondary aerosols could
104 lead to an severe haze event in China under certain meteorological conditions (Wang et
105 al., 2016;Sun et al., 2014;Quan et al., 2013).

106 In the rural area of NCP, biomass burning for domestic cooking and heating, and
107 agricultural waste disposal is an important source of atmospheric PM (Wang et al.,
108 2009b;Li et al., 2010;Zhang et al., 2016). Particularly, the open-field burning is still a
109 common way for disposal of crop residues (mainly wheat straw) in early summer (Li
110 et al., 2007). This traditional activity could release huge amounts of pollutants into the
111 atmosphere and significantly affect air quality and aerosol properties in the region.
112 Zhu et al. (2016) examined the amounts of VOCs in the air at a rural site of Yucheng
113 (Shandong Province, East China), and found that their concentrations during the
114 wheat straw burning period are approximately twice of those in normal periods.
115 Model results also revealed a significant influence of open crop residual burning ~~of~~

116 ~~erop-residual~~ on ozone, CO, black carbon (BC) and organic carbon (OC)
117 concentrations in NCP. Moreover, both off-line (Fu et al., 2012; Wang et al.,
118 2009b; Wang et al., 2011) and on-line (Sun et al., 2016) observations indicated that the
119 intensive emission from wheat straw burning in the region could change the molecular
120 distribution of organic aerosols ~~of~~ in the downwind urban or mountain areas.

121 During June 10th to 25th of 2013, we conducted a continuous sampling campaign
122 at a rural site in the northern part of NCP. PM_{2.5} filter samples were collected with a
123 3-hour time resolution and determined for more than 100 organic compounds
124 including aliphatic lipids, sugar compounds, hopanes, polycyclic aromatic
125 hydrocarbons (PAHs), phthalate esters, and secondary oxidation products. The first
126 objective of this study was to get an overall understanding of temporal/diurnal
127 variation and molecular distribution of summertime OA in the rural region. The
128 second objective was to compare the results in two representative periods to
129 investigate the influence of regional field burning of wheat straw on the molecular
130 characteristics of organic aerosols.

131 **2. Experimental section**

132 **2.1 Sample collection**

133 The sampling was performed at the Integrated Ecological-Meteorological
134 Observation and Experiment Station of Chinese Academy of Meteorological Sciences
135 (39°08' N, 115°40' E, 15.2 m a.s.l.), which is located in a rural area of Gucheng,
136 Hebei Province. Detailed information of the station and sampling campaign was
137 described in Li et al. (2018). Briefly, time-resolved (06:00–09:00, 09:00–12:00,

138 12:00–15:00, 15:00–18:00, 18:00–21:00, 21:00–24:00, 00:00–03:00, and 03:00–
139 06:00, Beijing time) PM_{2.5} samples were collected on the rooftop (about 10 m above
140 the ground) of a three-story building on the campus of the Gucheng station. The
141 sampling was conducted by using a high volume (1.13 m³ min⁻¹) sampler (Anderson)
142 with a PM_{2.5} inlet from June 10th to 25th, 2013. This period was chosen, because open-
143 field burning of wheat straw in NCP mainly occur in the mid of June. All samples
144 were collected onto pre-baked (450 °C, 6-8 hr) quartz fiber filters. Field blank samples
145 were also collected by mounting blank filters onto the sampler for about 15 min
146 without pumping any air. After sampling, the sample filter was individually sealed in
147 aluminum foil bags and stored in a freezer (-20 °C) prior to analysis.

148 **2.2 Organic compounds determination**

149 A size of 12.5-25 cm² of the filter sample was cut and extracted with a mixture of
150 dichloromethane and methanol (2:1, v/v) under ultrasonication. The extracts were
151 concentrated using a rotary evaporator under vacuum conditions and then blow down
152 to dryness using pure nitrogen. After reaction with N,O-bis-(trimethylsilyl)
153 trifluoroacetamide (BSTFA) at 70 °C for 3 hrs., the derivatives were determined
154 using gas chromatography/electron ionization mass spectrometry (GC/EI-MS) (Li et
155 al., 2013b).

156 GC/EI-MS analysis of the derivatized fraction was performed using an Agilent
157 7890A GC coupled with an Agilent 5975C MSD. The GC separation was carried out
158 on a DB-5MS fused silica capillary column with the GC oven temperature
159 programmed from 50°C (2 min) to 120°C at 15°C min⁻¹ and then to 300°C at 5°C

160 min⁻¹ with a final isothermal hold at 300 °C for 16 min. The sample was injected in a
161 splitless mode at an injector temperature of 280 °C, and scanned from 50 to 650
162 Daltons using electron impact (EI) mode at 70 eV.

163 GC/EI-MS response factors of all the target compounds were determined using
164 authentic standards except several isoprene-derived SOA tracers. Response factors of
165 isoprene-derived SOA tracers were substituted by those of related surrogated
166 standards, which were described in Li et al. (2018). No significant contamination
167 (<5% of those in the samples) was found in the blanks. Recoveries of all the target
168 compounds ranged from 80% to 120%. Data presented were corrected for the field
169 blanks but not corrected for the recoveries.

170 **2.3 OC, EC, and WSOC analysis**

171 OC (organic carbon) and EC (elemental carbon) were analyzed using DRI Model
172 2001 Carbon Analyzer following the Interagency Monitoring of Protected Visual
173 Environments (IMPROVE) thermal/optical reflectance (TOR) protocol. A size of
174 0.526 cm² sample filter was placed in a quartz boat inside the analyzer and stepwise
175 heated to temperatures of 140 °C (OC1), 280 °C (OC2), 480 °C (OC3), and
176 580 °C (OC4) in a non-oxidizing helium (He) atmosphere, and 580 °C (EC1),
177 740 °C (EC2), and 840 °C (EC3) in an oxidizing atmosphere of 2% oxygen in
178 helium. Pyrolyzed carbon (PC) is determined by reflectance and transmittance of 633
179 nm light. One sample was randomly selected from every 10 samples and re-analyzed.
180 Differences determined from the replicate analyses were <5% for TC, and <10% for
181 OC and EC.

182 Another aliquot of filter sample was extracted with organic-free Milli-Q water
183 under ultrasonication (15 min each, repeated 3 times) and filtered through a PTFE
184 filter to remove any particles and filter debris. Then the water-extract was analyzed
185 for water-soluble organic carbon (WSOC) using a TOC analyzer (TOC-L CPH,
186 Shimadzu, Japan). The difference between OC and WSOC was considered as water-
187 insoluble OC (WIOC). All carbonaceous components data reported here were
188 corrected by the field blanks.

189 **3. Results and discussion**

190 **3.1 Fire spots and air masses**

191 At present, open-field burning is still a common activity for disposal of crop
192 residue in the rural area of the North China Plain, especially during wheat harvest period
193 from the end of May to the middle of June (Fu et al., 2012). These extensive emissions
194 from regional biomass burning in the provinces of Anhui, Jiangsu, Shandong, Henan
195 and Hebei in NCP can cause severe air pollution on a local and regional scale. In our
196 previous study, the fire spots in NCP during the sampling period were provided based
197 on the NASA satellite observation (<https://firms.modaps.eosdis.nasa.gov/firemap/>).
198 Combining with information on air mass back-trajectories
199 (<http://ready.arl.noaa.gov/HYSPLIT.php>), the sampling period was divided into two
200 sections: (1) June 10-18, when air masses were mainly transported via long distances
201 from the southeast part of NCP, where intensive emissions from wheat straw burning
202 occurred; (2) June 19-25, when air masses were mostly influenced by local emissions
203 and regional emission from biomass burning decreased dramatically (Li et al., 2018).

204 In this study, we further selected two representative periods to estimate the contribution
205 of regional biomass burning. Period 1 (P1) designates 13th Jun 21:00 pm to 16th Jun
206 15:00 pm, during which air masses were influenced by intensive biomass burning and
207 transported uniformly from the southeast part of NCP (Figure 1 a and b, and Figure S1).
208 Period 2 (P2) designates 22nd Jun 12:00 pm to 24th Jun 06:00 am, during which fire
209 spots in the regions were relatively scarce and air masses came predominantly from the
210 surrounding areas of the sampling site (Figure 1 c and d). In addition, there were several
211 intermittent rainfalls during June 20th-22nd, which are favorable for wet deposition of
212 atmospheric pollutants. Thus, aerosols collected in P2 are well representative of local
213 fresh emission. It is worthwhile to note that the two samples collected during 21st June
214 18:00-24:00 pm were excluded from P2, because they were highly affected by near-site
215 biomass burning emission (detailed information is provided in Section 3.3).

216 3.2 Concentrations of PM_{2.5}, OC, EC, WSOC and WIOC

217 Concentrations of PM_{2.5} and carbonaceous components are presented in Table 1.
218 PM_{2.5} concentrations range from 21 to 395 $\mu\text{g m}^{-3}$ with a mean value at $159 \pm 89 \mu\text{g}$
219 m^{-3} during the whole sampling period. As shown in Figure 2, PM_{2.5} concentrations in
220 P1 (average $\pm 1\sigma = 231 \pm 89 \mu\text{g m}^{-3}$) increase continuously from around 150 μg
221 m^{-3} to higher than 300 $\mu\text{g m}^{-3}$, indicating the occurrence of a severe air pollution
222 episode. In contrast, PM_{2.5} concentration during P2 is as low as $43 \pm 14 \mu\text{g m}^{-3}$.
223 Similarly, the average concentration of OC is $29.4 \pm 7.8 \mu\text{g m}^{-3}$ in P1, which is more
224 than 5 time higher than that in P2 ($5.5 \pm 1.7 \mu\text{g m}^{-3}$). EC concentrations also
225 decrease dramatically from P1 ($12.1 \pm 4.0 \mu\text{g m}^{-3}$) to P2 ($1.5 \pm 1.5 \mu\text{g m}^{-3}$). The

设置了格式: 上标

226 average OC/EC ratio is 3.0 ± 0.9 for the whole sampling period, but the ratio in P2
227 (3.8 ± 1.0) ~~was is~~ higher ~~in P2 (3.8 ± 1.0)~~ than that in P1 (2.5 ± 0.4), mainly due to the
228 high SOA formation activities in the rural areas of NCP in summer. It's worthwhile to
229 note that the average OC/EC ratio during the BB-influenced P1 is much lower than
230 the results reported for wheat straw burning in combustion chamber (12.9 ± 2.1) (Tian
231 et al., 2017) ~~or~~ and residential stove ($6.3-11.1$) (Li et al., 2009). The first reason is that
232 fossil fuel burning (such as coal burning and vehicle exhaust) with lower OC/EC ratio
233 (Tian et al., 2017) are still important sources in the region, which are also discussed in
234 Section 3.4. On the other hand, this phenomenon may also be related to different
235 combustion conditions of agricultural residuals in the open field. Li et al. (2009)
236 found that the flaming fire from biomass burning would result in more EC emission
237 and lower OC/EC ratio compared to smoldering fire. Actually, Hays et al. (2005)
238 obtained similar low OC/EC ratio of 2.4 for open wheat straw burning smoke from
239 Washington, US. Thus, the lower ratio of OC/EC observed in this work may indicate
240 that wheat straw combustion in NCP during P1 mainly occurred ~~mainly~~ in the flaming
241 phase.

242 As shown in Figure 2 and 3, the concentrations of WSOC show a consistent
243 temporal variation as those of OC ($R^2=0.82$), highlighting the fact that WSOC is an
244 important fraction of OC in this region. In addition, the average ratio of WSOC/OC is
245 higher during P1 (0.62 ± 0.16) than during P2 (0.48 ± 0.12), mainly due to enhanced
246 emissions of water-soluble organic compounds (such as sugars, fatty alcohols/acids)
247 from biomass burning during P1. Due to the removal effect of the intermittent raining,

248 concentrations of water-insoluble OC in P2 ($3.0 \pm 1.3 \mu\text{g m}^{-3}$) are also much lower
249 than those in P1 ($10.3 \pm 4.4 \mu\text{g m}^{-3}$).

250 The diurnal variation profiles of EC/OC and WSOC/OC are shown in Figure 4.
251 EC/OC is generally lower in daytime and the lowest value occurred during 12:00-
252 15:00 pm, mainly due to enhanced daytime formation of SOC. Previous studies have
253 shown that ~~SOA~~secondary organic aerosols are mainly composed of water-soluble
254 compounds, e.g., polyacids/polyalcohols and phenols (Kondo et al., 2007; Wang et al.,
255 2009a). However, these compounds can ~~come be emitted~~ from primary emissions as
256 well, especially from biomass burning (Shen et al., 2017; Fu et al., 2012). In this study,
257 the WSOC/OC presents lower value during daytime, especially in the afternoon when
258 photo-chemical oxidation is favorable. In addition, the diurnal variation pattern of
259 WSOC/OC is similar to that of levoglucosan/OC. Given that levoglucosan is a marker
260 of biomass burning emissions (Simoneit et al., 1999; Simoneit et al., 2004a), and many
261 ~~kinds of~~ SOA could be produced in the biomass burning plumes during the long-range
262 transport (detailed discussions are given in Section 3.3). ~~these~~ These results indicate
263 that particulate WSOC in the region is mostly derived from biomass burning activities
264 including direct emission and secondary oxidation.

265 3.3 Organic molecular composition

266 More than 100 organic species were detected in the aerosol samples, and their
267 concentrations are shown in Table 2 and S1. In this study, these organic compositions
268 are grouped into 10 compound classes based on functional groups and sources. Total
269 concentrations of the measured organics ranged from 177 to 6248 ng m^{-3} (average =

270 $1806 \pm 1308 \text{ ng m}^{-3}$) during the whole sampling period with the predominance of
271 sugar compounds, followed by fatty acids and fatty alcohols. The temporal variation
272 profiles of the determined organic groups are shown in Figure 5. Nearly all the
273 measured organic species, especially *n*-alkanes, fatty acids, fatty alcohols, sugar
274 compounds, and PAHs, show much higher concentrations in P1 than in P2 (Figure
275 S2), indicating an important influence of regional biomass burning on airborne
276 organic aerosols in NCP.

277 3.3.1 Biomass-burning tracers

278 As described in Section 3.1, intensive emissions of open biomass burning were
279 observed in the southern part of NCP during June 13-16 (P1), which is an important
280 reason for the severe regional air pollution during this period. Levoglucosan, which is
281 produced in large quantities during pyrolysis of cellulose, is a key tracer for biomass
282 burning emissions (Simoneit, 2002; Simoneit et al., 1999). As shown in Table 2,
283 levoglucosan is the most abundant single compound in the whole sampling period,
284 ranged from 5.6 to 1447 ng m^{-3} with a mean concentration of $240 \pm 288 \text{ ng m}^{-3}$.
285 Levoglucosan shows good positive correlations with both OC ($R^2=0.61$) and WSOC
286 ($R^2=0.65$) (Figure 3), confirming that biomass burning is an important source of both
287 aerosol OC and WSOC in the rural region of NCP during the sampling period. As
288 clearly shown in Figure 6, the concentrations of levoglucosan present a continual
289 increasing trend during P1 with a mean value of $404 \pm 344 \text{ ng m}^{-3}$. However, the tracer
290 presents very low concentrations (11-123 ng m^{-3}) for ~~the~~ most of the time during Jun
291 20-22. Interestingly, the concentration of levoglucosan suddenly increased by more

292 than 10 times at 21st Jun 18:00 pm to approximately 1200 ng m⁻³ within less than 3
293 hours and then decreased to its beginning concentration (less than 100 ng m⁻³) within
294 6 hours (2 samples) afterwards. The concentrations of OC, WSOC and EC also
295 showed obvious peaks during this event. However, based on analyses of back-
296 trajectories (Figure 1c) and wind conditions (Figure S1), ~~we didn't find~~no significant
297 change of air mass origins was observed. Also, not all organic markers show~~ed~~
298 similar variations ~~as to~~ levoglucosan. For example, the concentrations of PAHs,
299 hopanes, and phthalate esters changed little during this event. Thus, it is plausible to
300 conclude that this variation was caused by emissions from biomass burning activities
301 nearby the sampling site. For this reason, the data of the 2 samples were excluded
302 from P2.

303 The two isomers of levoglucosan, galactosan and mannosan, are also produced
304 by the pyrolysis of cellulose/hemicelluloses (Simoneit, 2002), and thus also
305 considered as important markers of biomass burning. Similar to levoglucosan, the
306 concentrations of these two anhydrosugars in P1 are 5-6 times higher than those in P2.
307 The isomeric ratios of levoglucosan to other anhydrosugars are considered as good
308 indicators of biomass burning. Fabbri et al. (2009) compared the concentrations of the
309 three anhydrosaccharides in the smokes from different fuel types, and proposed that
310 levoglucan/(galactosan+mannosan) (L/G+M) and levoglucan/mannosan (L/M) values
311 range in 0.2-18 and 0.23-33 for various source tests for biomass burning as compared
312 to the average of 54 and 54 for lignites. As shown in Table 2, average ratios of L/G+M
313 and L/M during P1 (10.1 ± 3.41 and 6.77 ± 1.97 , respectively) and P2 (29.7 ± 12.2 and

314 18.0 ± 4.28) suggest that biomass burning is always the dominated contributor for
315 these compounds in the rural area of NCP in summer.

316 **3.3.2 Aliphatic lipid composition**

317 The average concentration of all the *n*-alkanes (C_{18} – C_{36}) measured in this study
318 is 207 ± 149 ng m^{-3} with the most abundant individual compound being nonacosane
319 ($C_{max}=C_{29}H_{60}$) (Table S1). *n*-Alkanes derived from terrestrial plants are dominated by
320 high molecular weight species (HMW, carbon number >25) with an odd number
321 preference. In contrast, fossil fuel derived *n*-alkanes do not have odd/even number
322 preference (Rogge et al., 1993a; Simoneit et al., 2004b). In general, *n*-alkanes with a
323 carbon preference index (CPI, odd/even) more than 5 are considered as plant wax,
324 while those with a CPI nearly unity are mostly derived from fossil fuel combustion
325 (Rogge et al., 1993a, b). In this study, the mean value of CPI is 2.47 ± 1.12 , indicating
326 that both fossil fuel and plant wax contributed to *n*-alkanes in the rural areas of NCP
327 in summer. However, *n*-alkanes showed a stronger odd/even carbon number
328 predominance in P1 (CPI=2.85) than in P2 (CPI=1.64). In addition, all the low
329 molecular weight *n*-alkanes (LMW, carbon number <25) presented a higher
330 contribution to total *n*-alkanes in P2 than in P1 (Figure 7 a and d). These results
331 demonstrate that plant waxes from biomass burning emissions made a bigger
332 contribution to organic aerosols in the sampling region during P1.

333 A homologous series of 19 saturated fatty acids ($C_{12:0}$ – $C_{32:0}$) and 3 unsaturated
334 fatty acids ($C_{16:1}$, $C_{18:1}$, and $C_{18:2}$) were detected in the samples (Table S1), and their
335 total concentration was 514 ± 384 ng m^{-3} during the whole period. A strong even

336 carbon number predominance ~~was~~is observed with C_{\max} at $C_{28:0}$ and $C_{16:0}$ (Table S1).
337 Higher molecular weight (HMW) fatty acids ($\geq C_{20}$) are derived from terrestrial plant
338 waxes, while LMW fatty acids ($\leq C_{19}$) have multiple sources such as vascular plants,
339 microbes and marine phytoplankton as well as kitchen emissions (Rogge et al.,
340 1993b; Kawamura et al., 2003). The total concentrations of fatty acids present~~ed~~
341 similar temporal variation to levoglucosan with a robust linear correlation ($R^2=0.72$)
342 (Figure 8a), indicating that fatty acids are mostly affected by biomass burning
343 emission during the whole sampling period. Still, there are some evidences that
344 regional emission from wheat straw burning significantly affected the distribution of
345 fatty acids in the aerosols of Gucheng during P1. Firstly, the total concentrations of
346 fatty acids in P1 ($900 \pm 358 \text{ ng m}^{-3}$) are more than 6 times higher than those in P2
347 ($145 \pm 48 \text{ ng m}^{-3}$). Secondly, the concentrations and relative contributions of HMW
348 fatty acids ($C_{20:0}$ – $C_{32:0}$) are much higher in P1 than in P2, similar to the results of *n*-
349 alkanes. In addition, the mean value of CPI of HMW fatty acids in P1 (4.21 ± 1.14) is
350 also higher than that in P2 (3.50 ± 1.64).

351 Fatty alcohols in the range of C_{22} – C_{30} were detected for the $PM_{2.5}$ samples with a
352 mean concentration of $193 \pm 187 \text{ ng m}^{-3}$ (Table 2 and S1) during the whole sampling
353 period. Their distributions are characterized by even carbon number predominance
354 with a maximum at C_{28} (Figure 7c and f). The total concentration of fatty alcohols
355 strongly ~~correlate~~correlates ~~d~~ with levoglucosan ($R^2=0.73$) (Figure 8b), suggesting
356 that they can also be emitted from biomass burning. It is reasonable since HMW fatty
357 alcohols ($\geq C_{20}$) abundantly present in higher plants and loess deposits (Wang and

358 Kawamura, 2005). Similar to fatty acids, nearly 10 times higher concentration of fatty
359 alcohols ~~was is~~ observed in P1 ($322 \pm 151 \text{ ng m}^{-3}$) compared with those in P2 (34 ± 23
360 ng m^{-3}).

361 **3.3.3 Primary saccharides**

362 In addition to the three anhydrosugars, 4 primary sugars (fructose, glucose, sucrose
363 and trehalose) and 3 sugar alcohols (arabitol, mannitol and inositol) were detected in
364 the samples. Primary saccharides have been used as biomarkers for primary biota
365 emissions (Wang et al., 2011). Their mean concentrations ranged from 3.6 to 49 ng m^{-3}
366 during the whole sampling period. In this study, concentrations of fructose, sucrose
367 and trehalose in P1 ~~were are~~ 7-10 times higher than those in P2 (Table S1). They well
368 correlated with levoglucosan ($R^2=0.47-0.62$, Figure S3) during P1, in contrast to P2,
369 during which no relationships ~~were are~~ found between them. These results indicated
370 that these primary sugars ~~were are~~ also affected by open-field emissions of biomass
371 burning during P1. Sugar alcohols, mainly arabitol and mannitol, are abundant in
372 airborne fungal spores (Graham et al., 2002). Some studies suggested that biomass
373 burning activities can enhance the emission of sugar alcohols at a certain level (Engling
374 et al., 2009;Fu et al., 2012;Yang et al., 2012). However, no significant relationship
375 ($R^2<0.10$) can be found between these sugar alcohols and levoglucosan even in P1,
376 indicating the negligible contribution of biomass burning to the tracers in this study.

377 **3.3.4 PAHs, Hopanes and Phthalates**

378 As shown in Figure 5, the temporal variation of PAHs, hopanes, and phthalate
379 esters were clearly different from those of the molecular tracers for biomass burning,

380 especially in P1. In contrast to the continuous increase of sugars, fatty acids, fatty
381 alcohols, and n-alkanes during P1, the concentrations of PAHs, hopanes, and phthalate
382 esters showed obvious day-night variations, indicating that biomass burning activities
383 contributed little on these species. Phthalates are widely used as plasticizers in synthetic
384 polymers or softeners in polyvinylchlorides (PVC) (Simoneit et al., 2004b) and can be
385 directly emitted from the matrix into the air as they are not chemically bonded with the
386 matrix. Six phthalate esters were detected in the sampling aerosols, i.e., dimethyl
387 (DMP), diethyl (DEP), diisobutyl (DiBP), butyl isobutyl (BiBP), di-n-butyl (DnBP),
388 and bis(2-ethylhexyl) (BEHP) phthalates (Table S1). The concentrations of total
389 detected phthalate esters in P1 ($112 \pm 33 \text{ ng m}^{-3}$) are around 2 times only higher than
390 those in P2 ($51 \pm 18 \text{ ng m}^{-3}$). Hopanes are abundant in coal and crude oils, and enriched
391 in lubricant oil fraction (Oros and Simoneit, 2000; Kawamura et al., 1995). They can be
392 emitted to the atmosphere from coal burning and/or internal combustion of fuel in
393 engines. Only two dominant hopanes, $17\alpha(\text{H}),21\beta(\text{H})$ -30-norhopane($\text{C}_{29\alpha\beta}$) and
394 $17\alpha(\text{H}),21\beta(\text{H})$ -hopane($\text{C}_{30\alpha\beta}$), were detected in all of the samples in this study. Their
395 average concentration in P1 ($4.40 \pm 2.48 \text{ ng m}^{-3}$) is ~ 2.5 times of that in P2 ($1.81 \pm$
396 0.31 ng m^{-3}). Considering the much higher concentrations of levoglucosan in P1 (on
397 average ~ 8 times higher than P2), these results again confirmed a limited influence of
398 biomass burning on concentrations of phthalate esters and hopanes in the aerosols in
399 the rural region. Thus, there were no significant concentration changes of the two
400 species at 21st Jun 18:00-24:00 pm, when the air masses were highly affected by nearby
401 biomass burning activities.

402 PAHs are the products of incomplete combustion of carbon-containing materials
403 and are of high toxicity and carcinogenicity (Halek et al., 2008;Sultan et al., 2001).
404 Previous studies indicated that PAHs are mainly emitted from coal burning and vehicle
405 exhaust in most areas of China (Wang et al., 2006a). However, it has been reported that
406 combustion of biomass materials can also contribute to the PAHs in the atmosphere
407 (Simoneit, 2002;Ge et al., 2012;Young et al., 2016). In this study, PAH has no
408 significant correlation with levoglucosan during the whole sampling period. Yet the
409 concentrations of total PAHs in P1 ($18.6 \pm 11 \text{ ng m}^{-3}$) are nearly 8 times higher than
410 those in P2 ($2.3 \pm 1.0 \text{ ng m}^{-3}$). These results ~~mean-suggest~~ that although the emission of
411 biomass burning is not the most important source for PAHs during the entire period, the
412 intensive regional burning of wheat straw in P1 can also enhance the PAHs
413 concentration in the atmosphere of Gucheng.

414 As shown in Figure 9, all the primary aerosol markers mentioned above showed
415 lower concentrations in daytime with lowest concentrations at afternoon (12:00-18:00
416 pm), in consistent with the favorable dispersion conditions caused by high temperature
417 and planetary boundary layer (PBL) height. However, the day-night variation of PAHs,
418 hopanes, and phthalate esters are more obvious than other species, again confirming the
419 lower contribution of biomass burning to these organic compositions.

420 **3.3.5 Secondary organic aerosols (SOA) tracers**

421 Eight compounds were identified as isoprene oxidation products in the $\text{PM}_{2.5}$
422 samples, including two methyltetrahydrofuran diols, three C_5 -alkene triols, two 2-
423 methyltetrols, and 2-methylglyceric acid (Table S1). Detailed information about

424 formation and contribution of these compositions were discussed in our previous paper
425 (Li et al., 2018). The concentrations of total detected isoprene-derived products are 112
426 $\pm 86 \text{ ng m}^{-3}$, with much higher concentration in P1 ($209 \pm 105 \text{ ng m}^{-3}$) than in P2 (57
427 $\pm 29 \text{ ng m}^{-3}$).

428 *cis*-Pinonic acid (PNA), pinic acid (PA), 3-hydroxyglutaric acid (HGA) and 3-
429 methyl-1,2,3-butanetricarboxylic acid (MBTCA) were detected as tracers for α -/ β -
430 pinene oxidation in this study, and their concentrations are shown in Table S1. The
431 concentration of total detected α -/ β -pinene oxidation tracers is $66 \pm 31 \text{ ng m}^{-3}$, with
432 MBTCA ($31 \pm 14 \text{ ng m}^{-3}$) being the major compound during the whole sampling period.
433 PNA and PA are considered as first-generation products of α -/ β -pinene oxidation. They
434 can be produced by further oxidation of carbonyl-substituted Criegee intermediates
435 formed by α -pinene ozonolysis (Jenkin et al., 2000; Ma et al., 2008), or by OH oxidation
436 of α -pinene under NO_x free conditions (Eddingsaas et al., 2012; Xuan et al., 2015). The
437 formation of 3-HGA is supposed to be based on a ring opening mechanism and may be
438 related to a heterogeneous reaction of these monoterpenes with irradiation in the
439 presence of NO_x (Jaoui et al., 2005; Claeys et al., 2007). As shown in Figure 6b-d, PNA,
440 PA and HGA present similar temporal variations and correlated well each other
441 ($R^2=0.48-0.76$, Figure S4). The formation of MBTCA is explained by further
442 photodegradation of *cis*-pinonic acid and pinic acid with OH radical (Müller et al.,
443 2012; Szmigielski et al., 2007). As a later-generation oxidation products, MBTCA
444 showed an obviously different temporal variation profile than those of PNA and PA,
445 and ~~had~~ has no significant increase during P1. In addition, the concentrations of PNA,

446 PA and HGA in P1 are 2-8 times higher than those in P2. However, the concentrations
447 of MBTCA in the two periods are comparable. These results are consistent with the
448 longer time scales of formation pathway, lower volatility and longer lifetime of
449 MBTCA in the atmosphere compared to the first-generation products of α -/ β -pinene
450 oxidation. β -Caryophyllinic acid, formed either by ozonolysis or photo-oxidation of β -
451 caryophyllene (a sesquiterpene) (Jaoui et al., 2007), was also determined in this study,
452 and its concentration ranged from 0.49 to 78 ng m⁻³ (Ave. 17±17 ng m⁻³). The mean
453 concentration of β -caryophyllinic acid in P1 is 35±21 ng m⁻³, being 5 times higher than
454 that in P2 (4.1±1.2 ng m⁻³).

455 Undoubtedly, the combustion of biomass materials can release a large amount of
456 ~~volatile organic compound~~VOCs, including isoprene and terpenoids (Andreae and
457 Merlet, 2001). As shown in Figure 5 and 6, ~~the~~ total biogenic SOA tracers, the sum of
458 detected tracers of isoprene, α -/ β -pinene, and β -caryophyllene derived SOA, showed a
459 similar temporal variation pattern as levoglucosan with a moderate correlation ($R^2=0.56$,
460 Figure S5a). Specifically, levoglucosan showed strong linearly correlations with 3-
461 hydroxyglutaric acid ($R^2=0.72$) (Figure 8c) and β -caryophyllinic acid ($R^2=0.80$) (Figure
462 8d), indicating a significant contribution of biomass burning emissions to the formation
463 of SOA derived from mono- and sesqui- terpene oxidation. In our previous paper (Li et
464 al., 2018), we discussed the different diurnal variations of isoprene-derived SOA tracers.
465 In this study, the diurnal variations of other SOA tracers are shown in Figure 10. All the
466 SOA tracers presented weaker day-night variations compared to primary organic
467 aerosol markers, because of the competition between the enhanced daytime formation

468 by photooxidation and the nighttime accumulation associated with a low PBL. Yet, there
469 are some differences between these SOA tracers. For example, PNA and PA presented
470 lowest concentrations in the afternoon (12:00-18:00 pm) due to their relatively high
471 volatilities, which is unfavorable for gas-to-particle phase partitioning. However, the
472 later-generation product of PNA and PA, i.e., the less volatile MBTCA, continuously
473 increases during the daytime.

474 Two classes of aromatic SOA markers, phthalic acids and 2,3-dihydroxy-4-
475 oxopentanoic acid (DHOPA), were detected in the samples as well. Phthalic acids are
476 believed to be produced by the oxidation of naphthalene and other PAHs (Kawamura
477 et al., 2005; Kawamura and Ikushima, 1993; Kanakidou et al., 2005). The mean
478 concentrations of total phthalic acids in the whole sampling period range from 17 to
479 487 ng m⁻³ with a mean value of 155±94 ng m⁻³. Their different temporal variation
480 patterns than levoglucosan suggest that biomass burning emission contributes little to
481 phthalic acids formation in the region. The DHOPA was considered to be a tracer
482 compound for toluene-derived SOA (Kleindienst et al., 2004). DHOPA presents a
483 similar temporal variation and a moderate correlation ~~to~~ with levoglucosan ($R^2=0.51$,
484 Figure S5b), indicating a certain contribution of biomass burning. Similar to MBTCA,
485 the volatility of DHOPA is quite low, and thus mainly exists in the particle phase at field
486 temperature (Ding et al., 2017). Thus, DHOPA shows a similar diurnal variation to
487 MBTCA, with higher concentrations during daytime.

488 3.4 Assessment of source contributions

489 In order to investigate the differences in organic aerosol sources between the two

490 representative periods, we classified all the measured organic compounds into seven
491 different sources: (a) “plant emission” represented by higher plant wax n-alkanes,
492 HMW fatty acids and fatty alcohols ($\geq C_{20}$); (b) “fossil fuel combustion” mainly
493 represented by fossil fuel derived n-alkanes, hopanes, and PAHs; (c) “biomass burning”
494 represented by levoglucosan and its isomers; (d) “marine/microbial source” represented
495 by LMW fatty acids ($< C_{20}$); (e) “soil/fungal spore/pollen” represented by primary
496 saccharides and sugar alcohols; (f) “plastic emission” represented by phthalate esters;
497 and (g) “secondary oxidation” represented by biogenic SOA tracers, DHOPA, and
498 phthalic acids. The concentrations of individual classes and their contributions to OC
499 content during P1 and P2 are summarized in Figure 11. Plant emission-derived
500 compounds accounted for a larger fraction of $PM_{2.5}$ OC during P1 than during P2 (mean
501 fractions of $28.7 \pm 9.3\%$ in P1 vs. $16.5 \pm 7.2\%$ in P2). The average fraction of biomass
502 burning-derived organics in P1 ($6.0 \pm 3.9\%$) ~~was~~ is also higher ~~in P1~~ than that in P2
503 (~~$6.0 \pm 3.9\%$ vs. $4.6 \pm 2.1\%$~~), so do organics derived from soil/fungal spore/pollen.
504 However, organic molecules from the other 4 sources ~~presented~~ a higher contribution
505 to OC in P2 than in P1.

506 Since organic compounds in the $PM_{2.5}$ samples cannot be completely determined
507 and some of them are of different sources, thus the above classification based on the
508 measured compounds could result in certain uncertainty in assessing source
509 contributions (Simoneit et al., 2004b). Here, we further used a tracer-based source
510 apportionment method to quantitatively estimate the contributions of primary and
511 secondary sources to the fine particulate OC at the rural site. As described above, two

512 samples collected at 21st Jun 18:00-24:00 pm were considered to be highly affected by
513 the direct emission from biomass burning nearby the sampling site. Thus, the average
514 OC/levoglucosan ratio in the smoke of biomass burning $\left(\frac{OC}{Levo}\right)_{BB}$ can be estimated
515 by using the following equation:

$$516 \quad \left(\frac{OC}{Levo}\right)_{BB} = \frac{OC_n - \frac{1}{2}(OC_{before} + OC_{after})}{Levo_n - \frac{1}{2}(Levo_{before} + Levo_{Levo})} \quad (E1)$$

517 where OC_n and $Levo_n$ are the average concentrations of OC and levoglucosan in
518 the two PM_{2.5} samples affected by the nearby sources. OC_{before} and $Levo_{before}$ are the
519 concentrations of OC and levoglucosan in the samples collected before the event, while
520 OC_{after} and $Levo_{after}$ are the concentrations of OC and levoglucosan in the samples
521 collected after the event. The mean values in the “before” and the “after” samples were
522 subtracted to minimize the influence of local background contribution. The calculated
523 $\left(\frac{OC}{Levo}\right)_{BB}$ in this study is 18.7, which is somewhat higher than the average value of 12.1
524 measured in PM_{2.5} aerosols emitted from the burning of three types of cereal straws
525 (i.e., wheat, maize, and rice) in China (Zhang et al., 2007b). This difference can be
526 attributed to the differences of burning conditions. For other sources, the measured
527 concentrations of mannitol were used to calculate the contributions of fungal spores to
528 OC (Bauer et al., 2008), and SOA tracers were used to estimate the SOC formed from
529 the oxidation of isoprene, α -/ β -pinene, β -caryophyllene, and toluene (Kleindienst et al.,
530 2007). Also, these tracer-based approaches tend to have large uncertainties, especially
531 for SOC estimation (Li et al., 2013a). However, our results are still meaningful to
532 understand the relative abundances of organic aerosols from these sources in different
533 periods.

534 As shown in Figure 12, biomass-burning derived OC, ranging from 0.11-27.5 μgC
535 m^{-3} , is the dominant source, which accounts for 1.16-74.8% (ave. 22.6%) of OC in the
536 aerosols of the rural region during the whole sampling period. Fungal-spore derived OC
537 (0.003-5.12 $\mu\text{gC m}^{-3}$) is a minor source, only accounting for 0.43% (0.003-5.12%) of
538 OC. The contribution of total SOC derived from oxidation of isoprene, α -/ β -pinene, β -
539 caryophyllene, and toluene to OC ranged from 5.90-34.1% with an average ~~at~~ of 16.7%.
540 Among the four SOC precursors, toluene-derived products accounted ~~ed~~ for 7.78% (2.06-
541 21.7%) of OC, being the most important SOC contributor. The relative abundances of
542 these sources showed ~~ed~~ clear temporal variations during the whole sampling period
543 (Figure 12). The contribution of biomass burning derived OC to total OC in P1 (27.6%)
544 ~~is~~ was 1.7 times of that in P2 (17.1%) (Figure 13), further indicating the strong regional
545 impact of open-field wheat straw burning on the molecular compositions of organic
546 aerosols in the rural area of NCP. The contribution of SOC from oxidation of the four
547 VOCs increase ~~d~~ slightly from P1 (16.3%) to P2 (21.1%). It should be noted that
548 biomass burning can also release a large amount of VOCs, which may produce more
549 secondary organic aerosols during the long-range transport. Thus, the impact of
550 intensive biomass burning in the southern region of NCP on organic aerosols in the
551 Gucheng area is likely even stronger than the estimation presented above with
552 implications for regional climate.

553 4. Summary and Conclusion

554 During the entire sampling period, OC and WSOC showed strong positive
555 correlations with levoglucosan, and the diurnal variation of WSOC/OC was similar to

556 that of levoglucosan/OC, suggesting that summertime organic aerosols in the rural
557 area of NCP are highly affected by direct emission of BB. Higher relative abundances
558 and CPI values of HMW n-alkanes, fatty acids and fatty alcohols in P1 indicated an
559 ~~enhancing~~ enhanced effect of open-field biomass burning on molecular composition
560 of organic aerosols. PAHs, hopanes, and phthalate esters presented different temporal
561 and diurnal variations ~~from to~~ levoglucosan because of the lower contribution of BB
562 to these organic compositions. The total biogenic SOA tracers showed a similar
563 temporal variation and a moderate correlation with levoglucosan, demonstrating the
564 enhancing effect of BB emission on BSOA formation. Later-generation SOA
565 products, e.g., MBTCA in this study, ~~are~~ were unlikely affected directly by BB
566 emission, and thus showed little changes in concentrations between the two periods.
567 The source distribution results derived using a tracer-based method demonstrated that
568 the contribution of BB to organic aerosols increased by more than 50% during the
569 period influenced by regional open-field biomass burning (P1) compared to the period
570 when local emissions were more dominant (P2). However, this contribution may even
571 be underestimated since BB can also release a large amount of VOCs enhancing the
572 formation of SOA in the atmosphere. Our results confirmed that intensive field
573 burning of biomass fuels can significantly influence the concentration and
574 composition of aerosols, and thus affect atmospheric chemistry and climate on a
575 regional scale.

576

577 **Author Contributions**

578 G.H. Wang designed the experiment. G.H. Wang, T. Zhu and L.M. Zeng arranged the

579 sample collection. J.J. Li. and G.H. Wang collected the samples. J.J. Li, G.H. Wang, J.
580 Li, C. Wu and W.Q. Jiang analyzed the samples. J.J. Li, and G.H. Wang performed the
581 data interpretation. J.J. Li, G.H. Wang and Q. Zhang wrote the paper.
582
583

584 **Acknowledgements**

585 This work was financially supported by the program from National Nature Science
586 Foundation of China (No. 41773117, 91543116, 41405122). The authors gratefully
587 acknowledge the use of fire spots data products from the Land, Atmosphere Near real-
588 time Capability for EOS (LANCE) system operated by the NASA/GSFC/Earth
589 Science Data and Information System (ESDIS) with funding provided by NASA/HQ
590 (<https://firms.modaps.eosdis.nasa.gov/firemap/>), and the NOAA Air Resources
591 Laboratory (ARL) for the provision of the HYSPLIT transport and dispersion model
592 and/or READY website (<http://www.ready.noaa.gov>) used in this publication.
593
594
595

596 **Reference**

- 597 Aggarwal, S. G., Kawamura, K., Umarji, G. S., Tachibana, E., Patil, R. S., and Gupta, P. K.: Organic and
598 inorganic markers and stable C-, N-isotopic compositions of tropical coastal aerosols from megacity
599 Mumbai: sources of organic aerosols and atmospheric processing, *Atmos. Chem. Phys.*, 13, 4667-
600 4680, 10.5194/acp-13-4667-2013, 2013.
- 601 Andreae, M. O., and Merlet, P.: Emission of trace gases and aerosols from biomass burning, *Global*
602 *Biogeochemical Cycles*, 15, 955-966, 10.1029/2000gb001382, 2001.
- 603 Andreae, M. O., and Rosenfeld, D.: Aerosol-cloud-precipitation interactions. Part 1. The nature and
604 sources of cloud-active aerosols, *Earth-Science Reviews*, 89, 13-41,
605 10.1016/j.earscirev.2008.03.001, 2008.
- 606 Chan, M. N., Choi, M. Y., Ng, N. L., and Chan, C. K.: Hygroscopicity of water-soluble organic
607 compounds in atmospheric aerosols: Amino acids and biomass burning derived organic species,
608 *Environ. Sci. Technol.*, 39, 1555-1562, 10.1021/es049584l, 2005.
- 609 Claeys, M., Szmigielski, R., Kourtev, I., Van der Veken, P., Vermeylen, R., Maenhaut, W., Jaoui, M.,
610 Kleindienst, T. E., Lewandowski, M., Offenberg, J. H., and Edney, E. O.: Hydroxydicarboxylic
611 Acids: Markers for Secondary Organic Aerosol from the Photooxidation of α -Pinene, *Environ. Sci.*
612 *Technol.*, 41, 1628-1634, 10.1021/es0620181, 2007.
- 613 Dinar, E., Anttila, T., and Rudich, Y.: CCN activity and hygroscopic growth of organic aerosols following
614 reactive uptake of ammonia, *Environ. Sci. Technol.*, 42, 793-799, 10.1021/es071874p, 2008.
- 615 Ding, X., Zhang, Y. Q., He, Q. F., Yu, Q. Q., Wang, J. Q., Shen, R. Q., Song, W., Wang, Y. S., and Wang,
616 X. M.: Significant Increase of Aromatics-Derived Secondary Organic Aerosol during Fall to Winter
617 in China, *Environ. Sci. Technol.*, 51, 7432-7441, 10.1021/acs.est.6b06408, 2017.
- 618 Eddingsaas, N. C., Loza, C. L., Yee, L. D., Chan, M., Schilling, K. A., Chhabra, P. S., Seinfeld, J. H., and
619 Wennberg, P. O.: α -pinene photooxidation under controlled chemical conditions - Part 2: SOA
620 yield and composition in low- and high-NO_x environments, *Atmos. Chem. Phys.*, 12, 7413-7427,
621 10.5194/acp-12-7413-2012, 2012.
- 622 Engling, G., Lee, J. J., Tsai, Y. W., Lung, S. C. C., Chou, C. C. K., and Chan, C. Y.: Size-Resolved
623 Anhydrosugar Composition in Smoke Aerosol from Controlled Field Burning of Rice Straw,
624 *Aerosol Science and Technology*, 43, 662-672, 10.1080/02786820902825113, 2009.
- 625 Fabbri, D., Torri, C., Simoneit, B. R. T., Marynowski, L., Rushdi, A. I., and Fabiańska, M. J.:
626 Levoglucosan and other cellulose and lignin markers in emissions from burning of Miocene lignites,
627 *Atmos. Environ.*, 43, 2286-2295, 2009.
- 628 Fu, P. Q., Kawamura, K., Pavuluri, C. M., Swaminathan, T., and Chen, J.: Molecular characterization of
629 urban organic aerosol in tropical India: contributions of primary emissions and secondary
630 photooxidation, *Atmos. Chem. Phys.*, 10, 2663-2689, 2010.
- 631 Fu, P. Q., Kawamura, K., Chen, J., Li, J., Sun, Y. L., Liu, Y., Tachibana, E., Aggarwal, S. G., Okuzawa,

632 K., Tanimoto, H., Kanaya, Y., and Wang, Z. F.: Diurnal variations of organic molecular tracers and
633 stable carbon isotopic composition in atmospheric aerosols over Mt. Tai in the North China Plain:
634 an influence of biomass burning, *Atmos. Chem. Phys.*, 12, 8359-8375, 10.5194/acp-12-8359-2012,
635 2012.

636 Ge, X., Setyan, A., Sun, Y., and Zhang, Q.: Primary and secondary organic aerosols in Fresno, California
637 during wintertime: Results from high resolution aerosol mass spectrometry, *Journal of Geophysical
638 Research: Atmospheres*, 117, n/a-n/a, 10.1029/2012jd018026, 2012.

639 Graham, B., Mayol-Bracero, O. L., Guyon, P., Roberts, G. C., Decesari, S., Facchini, M. C., Artaxo, P.,
640 Maenhaut, W., Koll, P., and Andreae, M. O.: Water-soluble organic compounds in biomass burning
641 aerosols over Amazonia - 1. Characterization by NMR and GC-MS, *J. Geophys. Res.-Atmos.*, 107,
642 DOI:804710.801029/802001jd000336, 2002.

643 Guo, S., Hu, M., Zamora, M. L., Peng, J., Shang, D., Zheng, J., Du, Z., Wu, Z., Shao, M., Zeng, L.,
644 Molina, M. J., and Zhang, R.: Elucidating severe urban haze formation in China, *Proceedings of the
645 National Academy of Sciences of the United States of America*, 111, 17373-17378,
646 10.1073/pnas.1419604111, 2014.

647 Halek, F., Nabi, G., and Kavousi, A.: Polycyclic aromatic hydrocarbons study and toxic equivalency
648 factor (TEFs) in Tehran, IRAN, *Environmental Monitoring and Assessment*, 143, 303-311,
649 10.1007/s10661-007-9983-9, 2008.

650 Hallquist, M., Wenger, J. C., Baltensperger, U., Rudich, Y., Simpson, D., Claeys, M., Dommen, J.,
651 Donahue, N. M., George, C., Goldstein, A. H., Hamilton, J. F., Herrmann, H., Hoffmann, T., Iinuma, Y.,
652 Jang, M., Jenkin, M. E., Jimenez, J. L., Kiendler-Scharr, A., Maenhaut, W., McFiggans, G.,
653 Mentel, T. F., Monod, A., Prevot, A. S. H., Seinfeld, J. H., Surratt, J. D., Szmigielski, R., and Wildt,
654 J.: The formation, properties and impact of secondary organic aerosol: current and emerging issues,
655 *Atmos. Chem. Phys.*, 9, 5155-5236, 2009.

656 Hays, M. D., Fine, P. M., Geron, C. D., Kleeman, M. J., and Gullett, B. K.: Open burning of agricultural
657 biomass: Physical and chemical properties of particle-phase emissions, *Atmos. Environ.*, 39, 6747-
658 6764, <https://doi.org/10.1016/j.atmosenv.2005.07.072>, 2005.

659 Huang, R. J., Zhang, Y. L., Bozzetti, C., Ho, K. F., Cao, J. J., Han, Y. M., Daellenbach, K. R., Slowik, J.
660 G., Platt, S. M., Canonaco, F., Zotter, P., Wolf, R., Pieber, S. M., Bruns, E. A., Crippa, M., Ciarelli,
661 G., Piazzalunga, A., Schwikowski, M., Abbaszade, G., Schnelle-Kreis, J., Zimmermann, R., An, Z.
662 S., Szidat, S., Baltensperger, U., El Haddad, I., and Prevot, A. S. H.: High secondary aerosol
663 contribution to particulate pollution during haze events in China, *Nature*, 514, 218-222,
664 10.1038/nature13774, 2014.

665 Jaoui, M., Kleindienst, T. E., Lewandowski, M., Offenberg, J. H., and Edney, E. O.: Identification and
666 quantification of aerosol polar oxygenated compounds bearing carboxylic or hydroxyl groups. 2.
667 Organic tracer compounds from monoterpenes, *Environ. Sci. Technol.*, 39, 5661-5673,
668 10.1021/es048111b, 2005.

669 Jaoui, M., Lewandowski, M., Kleindienst, T. E., Offenberg, J. H., and Edney, E. O.: β -caryophyllinic
670 acid: An atmospheric tracer for β -caryophyllene secondary organic aerosol, *Geophysical Research
671 Letters*, 34, doi:10.1029/2006GL028827, 2007.

672 Jenkin, M. E., Shallcross, D. E., and Harvey, J. N.: Development and application of a possible mechanism
673 for the generation of cis-pinic acid from the ozonolysis of α - and β -pinene, *Atmos. Environ.*, 34,
674 2837-2850, 2000.

675 Jimenez, J. L., Canagaratna, M. R., Donahue, N. M., Prevot, A. S. H., Zhang, Q., Kroll, J. H., Decarlo,
676 P. F., Allan, J. D., Coe, H., and Ng, N. L.: Evolution of organic aerosols in the atmosphere, *Science*,
677 326, 1525-1529, 2009.

678 Kanakidou, M., Seinfeld, J. H., Pandis, S. N., Barnes, I., Dentener, F. J., Facchini, M. C., Van Dingenen,
679 R., Ervens, B., Nenes, A., Nielsen, C. J., Swietlicki, E., Putaud, J. P., Balkanski, Y., Fuzzi, S., Horth,
680 J., Moortgat, G. K., Winterhalter, R., Myhre, C. E. L., Tsigaridis, K., Vignati, E., Stephanou, E. G.,
681 and Wilson, J.: Organic aerosol and global climate modelling: a review, *Atmos. Chem. Phys.*, 5,
682 1053-1123, 2005.

683 Kawamura, K., and Ikushima, K.: Seasonal changes in the distribution of dicarboxylic acids in the urban
684 atmosphere, *Environ. Sci. Technol.*, 27, 2227-2235, 1993.

685 Kawamura, K., Kosaka, M., and Sempere, R.: Distributions and seasonal changes in hydrocarbons in
686 urban aerosols and rain waters, *Chikyu Kagaku (Geochemistry)*, 29, 1-15 (In Japanese), 1995.

687 Kawamura, K., Ishimura, Y., and Yamazaki, K.: Four years' observations of terrestrial lipid class
688 compounds in marine aerosols from the western North Pacific, *Global Biogeochemical Cycles*, 17,
689 10.1029/2001gb001810, 2003.

690 Kawamura, K., Imai, Y., and Barrie, L. A.: Photochemical production and loss of organic acids in high
691 Arctic aerosols during long-range transport and polar sunrise ozone depletion events, *Atmos.*

692 Environ., 39, 599-614, 10.1016/j.atmosenv.2004.10.020, 2005.

693 Kleindienst, T. E., Conner, T. S., McIver, C. D., and Edney, E. O.: Determination of secondary organic
694 aerosol products from the photooxidation of toluene and their implications in ambient PM_{2.5}, J.
695 Atmos. Chem., 47, 79-100, 2004.

696 Kleindienst, T. E., Jaoui, M., Lewandowski, M., Offenberg, J. H., Lewis, C. W., Bhavsar, P. V., and Edney,
697 E. O.: Estimates of the contributions of biogenic and anthropogenic hydrocarbons to secondary
698 organic aerosol at a southeastern US location, Atmos. Environ., 41, 8288-8300,
699 10.1016/j.atmosenv.2007.06.045, 2007.

700 Kondo, Y., Miyazaki, Y., Takegawa, N., Miyakawa, T., Weber, R. J., Jimenez, J. L., Zhang, Q., and
701 Worsnop, D. R.: Oxygenated and water-soluble organic aerosols in Tokyo, Journal of Geophysical
702 Research, 112, doi: 10.1029/2006jd007056, 10.1029/2006jd007056, 2007.

703 Lelieveld, J., Evans, J. S., Fnais, M., Giannadaki, D., and Pozzer, A.: The contribution of outdoor air
704 pollution sources to premature mortality on a global scale, Nature, 525, 367-371,
705 10.1038/nature15371, 2015.

706 Li, J. J., Wang, G. H., Cao, J. J., Wang, X. M., and Zhang, R. J.: Observation of biogenic secondary
707 organic aerosols in the atmosphere of a mountain site in central China: temperature and relative
708 humidity effects, Atmos. Chem. Phys., 13, 11535-11549, 10.5194/acp-13-11535-2013, 2013a.

709 Li, J. J., Wang, G. H., Wang, X. M., Cao, J. J., Sun, T., Cheng, C. L., Meng, J. J., Hu, T. F., and Liu, S.
710 X.: Abundance, composition and source of atmospheric PM_{2.5} at a remote site in the Tibetan
711 Plateau, China, Tellus B, 65, doi:10.3402/tellusb.v3465i3400.20281, 2013b.

712 Li, J. J., Wang, G. H., Wu, C., Cao, C., Ren, Y. Q., Wang, J. Y., Li, J., Cao, J. J., Zeng, L. M., and Zhu,
713 T.: Characterization of isoprene-derived secondary organic aerosols at a rural site in North China
714 Plain with implications for anthropogenic pollution effects, Scientific reports, 8, DOI:
715 10.1038/s41598-41017-18983-41597, 10.1038/s41598-017-18983-7, 2018.

716 Li, W. J., Shao, L. Y., and Buseck, P. R.: Haze types in Beijing and the influence of agricultural biomass
717 burning, Atmos. Chem. Phys., 10, 8119-8130, 10.5194/acp-10-8119-2010, 2010.

718 Li, X., Wang, S., Duan, L., Hao, J., and Nie, Y.: Carbonaceous Aerosol Emissions from Household
719 Biofuel Combustion in China, Environ. Sci. Technol., 43, 6076-6081, 10.1021/es803330j, 2009.

720 Li, Y. J., Sun, Y., Zhang, Q., Li, X., Li, M., Zhou, Z., and Chan, C. K.: Real-time chemical
721 characterization of atmospheric particulate matter in China: A review, Atmos. Environ., 158, 270-
722 304, 10.1016/j.atmosenv.2017.02.027, 2017.

723 Li, Z. Q., Xia, X. G., Cribb, M., Mi, W., Holben, B., Wang, P. C., Chen, H. B., Tsay, S. C., Eck, T. F.,
724 Zhao, F. S., Dutton, E. G., and Dickerson, R. R.: Aerosol optical properties and their radiative effects
725 in northern China, J. Geophys. Res.-Atmos., 112, 10.1029/2006jd007382, 2007.

726 Müller, L., Reining, M. C., Naumann, K. H., Saathoff, H., Mentel, T. F., Donahue, N. M., and Hoffmann,
727 T.: Formation of 3-methyl-1,2,3-butanetricarboxylic acid via gas phase oxidation of pinonic acid –
728 a mass spectrometric study of SOA aging, Atmos. Chem. Phys., 12, 1483-1496, 10.5194/acp-12-
729 1483-2012, 2012.

730 Ma, Y., Russell, A. T., and Marston, G.: Mechanisms for the formation of secondary organic aerosol
731 components from the gas-phase ozonolysis of alpha-pinene, Physical Chemistry Chemical Physics,
732 10, 4294-4312, 10.1039/b803283a, 2008.

733 Oros, D. R., and Simoneit, B. R. T.: Identification and emission rates of molecular tracers in coal smoke
734 particulate matter, Fuel, 79, 515-536, [http://dx.doi.org/10.1016/S0016-2361\(99\)00153-2](http://dx.doi.org/10.1016/S0016-2361(99)00153-2), 2000.

735 Quan, J. N., Gao, Y., Zhang, Q., Tie, X. X., Cao, J. J., Han, S. Q., Meng, J. W., Chen, P. F., and Zhao, D.
736 L.: Evolution of planetary boundary layer under different weather conditions, and its impact on
737 aerosol concentrations, Particuology, 11, 34-40, 10.1016/j.partic.2012.04.005, 2013.

738 Rogge, W. F., Hildemann, L. M., Mazurek, M. A., Cass, G. R., and Simoneit, B. R. T.: Sources of Fine
739 Organic Aerosols. 2. Noncatalyst and Catalyst-equipped Automobile and Heavy-duty Diesel Trucks,
740 Environ. Sci. Technol., 27, 636-651, 1993a.

741 Rogge, W. F., Hildemann, L. M., Mazurek, M. A., Cass, G. R., and Simoneit, B. R. T.: Sources of Fine
742 Organic Aerosols. 4. Particulate Abrasion Products from Leaf Surfaces of Urban Plants, Environ.
743 Sci. Technol., 27, 2700-2711, 1993b.

744 Shen, Z., Zhang, Q., Cao, J., Zhang, L., Lei, Y., Huang, Y., Huang, R. J., Gao, J., Zhao, Z., Zhu, C., Yin,
745 X., Zheng, C., Xu, H., and Liu, S.: Optical properties and possible sources of brown carbon in PM
746 2.5 over Xi'an, China, Atmos. Environ., 150, 322-330, 10.1016/j.atmosenv.2016.11.024, 2017.

747 Simoneit, B. R. T., Schauer, J. J., Nolte, C. G., Oros, D. R., Elias, V. O., Fraser, M. P., Rogge, W. F., and
748 Cass, G. R.: Levoglucosan, a tracer for cellulose in biomass burning and atmospheric particles,
749 Atmos. Environ., 33, 173-182, 1999.

750 Simoneit, B. R. T.: Biomass burning - A review of organic tracers for smoke from incomplete combustion,
751 Applied Geochemistry, 17, 129-162, 2002.

752 Simoneit, B. R. T., Elias, V. O., Kobayashi, M., Kawamura, K., Rushdi, A. I., Medeiros, P. M., Rogge,
753 W. F., and Didyk, B. M.: Sugars - Dominant water-soluble organic compounds in soils and
754 characterization as tracers in atmospheric particulate matter, *Environ. Sci. Technol.*, 38, 5939-5949,
755 10.1021/es0403099, 2004a.

756 Simoneit, B. R. T., Kobayashi, M., Mochida, M., Kawamura, K., Lee, M., Lim, H. J., Turpin, B. J., and
757 Komazaki, Y.: Composition and major sources of organic compounds of aerosol particulate matter
758 sampled during the ACE-Asia campaign, *J. Geophys. Res.-Atmos.*, 109, D19S10,
759 10.1029/2004jd004598, 2004b.

760 Sultan, C., Balaguer, P., Terouanne, B., Georget, V., Paris, F., Jeandel, C., Lumbroso, S., and Nicolas, J.
761 C.: Environmental xenoestrogens, antiandrogens and disorders of male sexual differentiation,
762 *Molecular and Cellular Endocrinology*, 178, 99-105, 10.1016/s0303-7207(01)00430-0, 2001.

763 Sun, Y. L., Jiang, Q., Wang, Z. F., Fu, P. Q., Li, J., Yang, T., and Yin, Y.: Investigation of the sources and
764 evolution processes of severe haze pollution in Beijing in January 2013, *J. Geophys. Res.-Atmos.*,
765 119, 4380-4398, 10.1002/2014jd021641, 2014.

766 Sun, Y. L., Jiang, Q., Xu, Y. S., Ma, Y., Zhang, Y. J., Liu, X. G., Li, W. J., Wang, F., Li, J., Wang, P. C.,
767 and Li, Z. Q.: Aerosol characterization over the North China Plain: Haze life cycle and biomass
768 burning impacts in summer, *J. Geophys. Res.-Atmos.*, 121, 2508-2521, 10.1002/2015jd024261,
769 2016.

770 Szmigielski, R., Surratt, J. D., Gomez-Gonzalez, Y., Van der Veken, P., Kourtchev, I., Vermeylen, R.,
771 Blockhuys, F., Jaoui, M., Kleindienst, T. E., Lewandowski, M., Offenberg, J. H., Edney, E. O.,
772 Seinfeld, J. H., Maenhaut, W., and Claeys, M.: 3-methyl-1,2,3-butanetricarboxylic acid: An
773 atmospheric tracer for terpene secondary organic aerosol, *Geophysical Research Letters*, 34, L24811,
774 10.1029/2007gl031338, 2007.

775 Tian, J., Ni, H. Y., Cao, J. J., Han, Y. M., Wang, Q. Y., Wang, X. L., Chen, L. W. A., Chow, J. C., Watson,
776 J. G., Wei, C., Sun, J., Zhang, T., and Huang, R. J.: Characteristics of carbonaceous particles from
777 residential coal combustion and agricultural biomass burning in China, *Atmospheric Pollution
778 Research*, 8, 521-527, 10.1016/j.apr.2016.12.006, 2017.

779 Tie, X. X., Huang, R. J., Dai, W. T., Cao, J. J., Long, X., Su, X. L., Zhao, S. Y., Wang, Q. Y., and Li, G.
780 H.: Effect of heavy haze and aerosol pollution on rice and wheat productions in China, *Scientific
781 reports*, 6, 10.1038/srep29612, 2016.

782 van Donkelaar, A., Martin, R. V., Brauer, M., Kahn, R., Levy, R., Verduzco, C., and Villeneuve, P. J.:
783 Global Estimates of Ambient Fine Particulate Matter Concentrations from Satellite-Based Aerosol
784 Optical Depth: Development and Application, *Environmental Health Perspectives*, 118, 847-855,
785 10.1289/ehp.0901623, 2010.

786 Venkataraman, C., Habib, G., Eiguren-Fernandez, A., Miguel, A. H., and Friedlander, S. K.: Residential
787 biofuels in south Asia: Carbonaceous aerosol emissions and climate impacts, *Science*, 307, 1454-
788 1456, 10.1126/science.1104359, 2005.

789 Wang, G. H., and Kawamura, K.: Molecular characteristics of urban organic aerosols from Nanjing: A
790 case study of a mega-city in China, *Environ. Sci. Technol.*, 39, 7430-7438, 10.1021/es051055+,
791 2005.

792 Wang, G. H., Kawamura, K., Lee, S., Ho, K. F., and Cao, J. J.: Molecular, seasonal, and spatial
793 distributions of organic aerosols from fourteen Chinese cities, *Environ. Sci. Technol.*, 40, 4619-
794 4625, 10.1021/es060291x, 2006a.

795 Wang, G. H., Kawamura, K., Watanabe, T., Lee, S. C., Ho, K. F., and Cao, J. J.: High loadings and source
796 strengths of organic aerosols in China, *Geophysical Research Letters*, 33,
797 L2280110.1029/2006gl027624, 2006b.

798 Wang, G. H., Kawamura, K., Umemoto, N., Xie, M. J., Hu, S. Y., and Wang, Z. F.: Water-soluble organic
799 compounds in PM_{2.5} and size-segregated aerosols over Mount Tai in North China Plain, *J. Geophys.
800 Res.-Atmos.*, 114, doi: 10.1029/2008jd011390, D1920810.1029/2008jd011390, 2009a.

801 Wang, G. H., Kawamura, K., Xie, M. J., Hu, S. Y., Cao, J. J., An, Z. S., Waston, J. G., and Chow, J. C.:
802 Organic Molecular Compositions and Size Distributions of Chinese Summer and Autumn Aerosols
803 from Nanjing: Characteristic Haze Event Caused by Wheat Straw Burning, *Environ. Sci. Technol.*,
804 43, 6493-6499, 10.1021/es803086g, 2009b.

805 Wang, G. H., Chen, C. L., Li, J. J., Zhou, B. H., Xie, M. J., Hu, S. Y., Kawamura, K., and Chen, Y.:
806 Molecular composition and size distribution of sugars, sugar-alcohols and carboxylic acids in
807 airborne particles during a severe urban haze event caused by wheat straw burning, *Atmos. Environ.*,
808 45, 2473-2479, 10.1016/j.atmosenv.2011.02.045, 2011.

809 Wang, G. H., Zhang, R. Y., Gomez, M. E., Yang, L. X., Zamora, M. L., Hu, M., Lin, Y., Peng, J. F., Guo,
810 S., Meng, J. J., Li, J. J., Cheng, C. L., Hu, T. F., Ren, Y. Q., Wang, Y. S., Gao, J., Cao, J. J., An, Z.
811 S., Zhou, W. J., Li, G. H., Wang, J. Y., Tian, P. F., Marrero-Ortiz, W., Secrest, J., Du, Z. F., Zheng,

812 J., Shang, D. J., Zeng, L. M., Shao, M., Wang, W. G., Huang, Y., Wang, Y., Zhu, Y. J., Li, Y. X., Hu,
813 J. X., Pan, B., Cai, L., Cheng, Y. T., Ji, Y. M., Zhang, F., Rosenfeld, D., Liss, P. S., Duce, R. A.,
814 Kolb, C. E., and Molina, M. J.: Persistent sulfate formation from London Fog to Chinese haze,
815 Proceedings of the National Academy of Sciences of the United States of America, 113, 13630-
816 13635, 10.1073/pnas.1616540113, 2016.

817 Xuan, Z., Renee C, M., Dan D, H., Nathan F, D., Bernard, A., Richard C, F., and John H, S.: Formation
818 and evolution of molecular products in α -pinene secondary organic aerosol, Proceedings of the
819 National Academy of Sciences of the United States of America, 112, 14168-14173, 2015.

820 Yang, Y. H., Chan, C. Y., Tao, J., Lin, M., Engling, G., Zhang, Z. S., Zhang, T., and Su, L.: Observation
821 of elevated fungal tracers due to biomass burning in the Sichuan Basin at Chengdu City, China,
822 Science of the Total Environment, 431, 68-77, 10.1016/j.scitotenv.2012.05.033, 2012.

823 Young, D. E., Kim, H., Parworth, C., Zhou, S., Zhang, X., Cappa, C. D., Seco, R., Kim, S., and Zhang,
824 Q.: Influences of emission sources and meteorology on aerosol chemistry in a polluted urban
825 environment: results from DISCOVER-AQ California, Atmos. Chem. Phys., 16, 5427-5451,
826 10.5194/acp-16-5427-2016, 2016.

827 Zhang, J. K., Cheng, M. T., Ji, D. S., Liu, Z. R., Hu, B., Sun, Y., and Wang, Y. S.: Characterization of
828 submicron particles during biomass burning and coal combustion periods in Beijing, China, The
829 Science of the total environment, 562, 812-821, 10.1016/j.scitotenv.2016.04.015, 2016.

830 Zhang, Q., Jimenez, J. L., Canagaratna, M. R., Allan, J. D., Coe, H., Ulbrich, I., Alfarra, M. R., Takami,
831 A., Middlebrook, A. M., and Sun, Y. L.: Ubiquity and dominance of oxygenated species in organic
832 aerosols in anthropogenically-influenced Northern Hemisphere midlatitudes, Geophysical Research
833 Letters, 34, L13801, 2007a.

834 Zhang, Q., Streets, D. G., Carmichael, G. R., He, K. B., Huo, H., Kannari, A., Klimont, Z., Park, I. S.,
835 Reddy, S., Fu, J. S., Chen, D., Duan, L., Lei, Y., Wang, L. T., and Yao, Z. L.: Asian emissions in
836 2006 for the NASA INTEX-B mission, Atmos. Chem. Phys., 9, 5131-5153, 10.5194/acp-9-5131-
837 2009, 2009.

838 Zhang, Y., Shao, M., Zhang, Y., Zeng, L., He, L., Zhu, B., Wei, Y., and Zhu, X.: Source profiles of
839 particulate organic matters emitted from cereal straw burnings, Journal of Environmental Sciences,
840 19, 167-175, [https://doi.org/10.1016/S1001-0742\(07\)60027-8](https://doi.org/10.1016/S1001-0742(07)60027-8), 2007b.

841 Zhu, Y., Yang, L., Chen, J., Wang, X., Xue, L., Sui, X., Wen, L., Xu, C., Yao, L., Zhang, J., Shao, M., Lu,
842 S., and Wang, W.: Characteristics of ambient volatile organic compounds and the influence of
843 biomass burning at a rural site in Northern China during summer 2013, Atmos. Environ., 124, 156-
844 165, 10.1016/j.atmosenv.2015.08.097, 2016.

845
846

847 Table 1 Concentrations of carbonaceous components in the time-resolved (3-h) PM_{2.5} samples in
 848 the rural site of NCP during the whole sampling period, Period 1 (P1) and Period 2 (P2).

Component	Whole period (N=117)			Period 1 (N=28)			Period 2 (N=13)		
	Range	Mean	SD	Range	Mean	SD	Range	Mean	SD
PM _{2.5} (µg m ⁻³)	21~395	159	89	133~347	231	59	21~62	43	14
OC (µg m ⁻³)	1.7~45.7	17.3	11.1	13.8~44.4	29.4	7.8	3.6~8.8	5.5	1.7
EC (µg m ⁻³)	0.2~22.3	6.5	4.9	5.3~22.3	12.1	4.0	0.9~2.6	1.5	0.5
WSOC (µg m ⁻³)	0.7~33.0	11.5	8.2	5.3~33.0	19.1	8.3	1.2~4.2	2.6	0.8
WIOC (µg m ⁻³)	0.3~28.1	6.4	5.1	4.5~28.1	10.3	4.4	1.2~5.5	3.0	1.3
OC/EC	1.2~7.6	3.0	0.9	1.9~3.2	2.5	0.4	2.5~5.7	3.8	1.0
WSOC/OC	0.07~0.95	0.63	0.18	0.30~0.85	0.62	0.16	0.18~0.67	0.48	0.12
WIOC/OC	0.05~0.93	0.37	0.18	0.15~0.70	0.38	0.16	0.33~0.82	0.52	0.12

849
 850
 851

852 Table 2 Average concentrations of the organic compound classes (ng m⁻³) in the time-resolved (3-h)
 853 PM_{2.5} samples in the rural site of NCP during the whole study period, Period 1 (P1) and Period 2
 854 (P2).

Compounds	Whole period (N=117)			Period 1 (N=28)			Period 2 (N=13)		
	Range	Mean	SD	Range	Mean	SD	Range	Mean	SD
n-Alkanes	9.97~722.2	206.9	149.3	94.7~722.3	343.7	134.1	25.1~103.2	54.3	22.4
CPI (C ₁₈ -C ₃₆) ^a	1.08~8.62	2.47	1.12	1.38~4.67	2.85	0.87	1.08~3.5	1.64	0.59
Fatty acids	64.6~1777	514.4	384.3	206.7~1528	900.3	358.3	81.4~234.4	145.3	47.7
CPI (C _{21:0} -C _{30:0}) ^b	2.26~9.15	4.24	1.14	3.49~6.11	4.21	0.64	2.26~8.57	3.50	1.64
Fatty alcohols	3.18~975.9	192.6	187.4	62.4~638.2	322.0	150.7	16.6~100.2	33.9	22.6
Sugar compounds	15.9~2228	432.8	428.9	151.9~1727	718.0	403.1	39.7~241.3	93.2	52.9
galactosan (G)	1.03~97.78	18.5	20.6	2.16~97.8	29.5	27.9	1.45~13.3	4.61	3.13
mannosan (M)	0.69~54.82	9.78	10.4	1.61~54.8	15.0	13.3	0.96~6.63	2.83	1.43
levoglucosan (L)	5.56~1447	240.1	287.8	29.3~1428	404.0	344.0	11.2~123	47.8	26.2
L/M ratio	4.03~71.8	22.8	8.85	13.9~71.8	29.7	12.2	11.3~23.1	18.0	4.28
L/(G+M) ratio	1.38~19.3	8.05	2.59	5.3~19.3	10.1	3.41	4.58~10.2	6.77	1.97
PAHs	1.11~48.5	12.0	11.0	4.21~37.7	18.6	11.0	1.25~5.01	2.33	0.98
Hopanes	0.66~10.81	3.46	2.38	0.86~9.97	4.40	2.48	1.14~2.28	1.81	0.31
Phthalate esters	17.7~219.9	84.9	41.3	68.8~183.1	111.5	32.7	31.5~100.8	51.1	18.1
Phthalic acids	17.1~487.2	154.5	93.9	91.3~388.6	211.0	87.1	17.1~81	46.3	17.1
Isoprene SOA tracers	11.1~404.1	111.9	85.8	48.3~404.1	208.5	104.9	34.8~127.5	57.0	29.4
Monoterpene SOA tracers	11.1~166.2	66.1	31.2	37.3~166.2	85.3	34.9	26.7~64.5	44.6	12.6
β-Caryophyllinic acid ^c	0.49~77.7	17.4	17.1	4.6~77.8	34.7	20.8	2.44~6.28	4.08	1.21
DHOPA ^d	1.59~35.3	9.36	7.15	4.06~35.3	15.6	9.80	2.7~6.99	4.16	1.42
Total measured organics	176.9~6249	1806	1308	843.3~5499	2973	1219	334.2~913.7	537.9	151.1
Total organics C/OC ^e (%)	3.19~16.0	6.99	1.97	3.43~8.86	6.43	1.36	3.77~8.61	6.41	1.27

855 ^a CPI (C₁₈-C₃₆): carbon preference index for *n*-alkanes, (C₁₉+C₂₁+C₂₃+C₂₅+C₂₇+C₂₉+C₃₁+C₃₃+C₃₅)/

856 (C₁₈+C₂₀+C₂₂+C₂₄+C₂₆+C₂₈+C₃₀+C₃₂+C₃₄).

857 ^b CPI (C_{21:0}-C_{30:0}): carbon preference index for fatty acids, (C_{22:0}+C_{24:0}+C_{26:0}+C_{28:0}+C_{30:0})/(C_{21:0}+C_{23:0}+C_{25:0}+C_{27:0}+C_{29:0}).

858 ^c β-Caryophyllinic acid: a tracer of β-caryophyllene-derived SOA.

859 ^d DHOPA: 2,3-dihydroxy-4-oxopentanoic acid, a tracer of toluene-derived SOA.

860 ^e All the quantified organic compounds were converted to their carbon contents to calculate the OC ratios.

861

Figure Captions

- 862 Figure 1. Backward trajectories of air masses (a,c) (provided by NOAA HYSPLIT modeling system,
863 <http://ready.arl.noaa.gov/HYSPLIT.php>), and fire spots (b,d) (provided by Fire Information
864 for Resource Management System, FIRMS, <https://firms.modaps.eosdis.nasa.gov/firemap/>),
865 during Period 1 (P1) (Jun 13th 21:00-16th 15:00, 2013) and Period 2 (P2) (Jun 22nd 12:00-24th
866 06:00, 2013). Sampling site represented as purple star.
- 867 Figure 2. Temporal variations of PM_{2.5}, OC, EC, and WSOC during the whole sampling period.
868 Shadows denote the two representative periods.
- 869 Figure 3. Linear correlations of OC with WSOC (a), levoglucosan with OC and WSOC(b).
- 870 Figure 4. Diurnal variation of OC/EC (a), WSOC/OC and levoglucosan/OC (b).
- 871 Figure 5. Temporal variations of ten organic compound classes detected in the summertime PM_{2.5}
872 samples at the rural site of NCP.
- 873 Figure 6. Temporal variations of organic tracers for biomass burning (a), and secondary products
874 derived from α - β -pinene (b-d), β -caryophyllene (e), and toluene (f).
- 875 Figure 7. Molecular distributions of *n*-alkanes (a and d), fatty acids (b and e), and fatty alcohols (c and
876 f) in the PM_{2.5} of the rural area.
- 877 Figure 8. Linear correlations of fatty acids (a), fatty alcohols (b), 3-hydroxyglutaric acid (c), and β -
878 caryophyllinic acid (d) with levoglucosan.
- 879 Figure 9. Diurnal variation of the detected organic compound classes.
- 880 Figure 10. Diurnal variation of the SOA tracers derived from oxidation of α - β -pinene (a-d), β -
881 caryophyllene (e), and toluene (f).
- 882 Figure 11. A comparison of the average contributions of different sources-derived organics (converted
883 to carbon content) to OC during P1 and P2.
- 884 Figure 12. Contributions (above) of primary organic carbon from biomass burning (OC_{bb}) and fungal
885 spores (OC_{fp}), and secondary organic carbon from isoprene (SOC_i), α - β -pinene (SOC_p), β -
886 caryophyllene (SOC_p), and toluene (SOC_t) to OC in the time-resolved (3 h) rural aerosols,
887 and their relative abundances (down). All the contributions were estimated by tracer-based
888 method.
- 889 Figure 13. Average contributions of direct emissions from biomass burning (BB) and fungal spores
890 (OC_{fp}), secondary oxidation from isoprene (SOC_i), α - β -pinene (SOC_p), β -caryophyllene
891 (SOC_p), and toluene (SOC_t) to OC in P1 and P2. All the contributions were estimated by
892 tracer-based method.

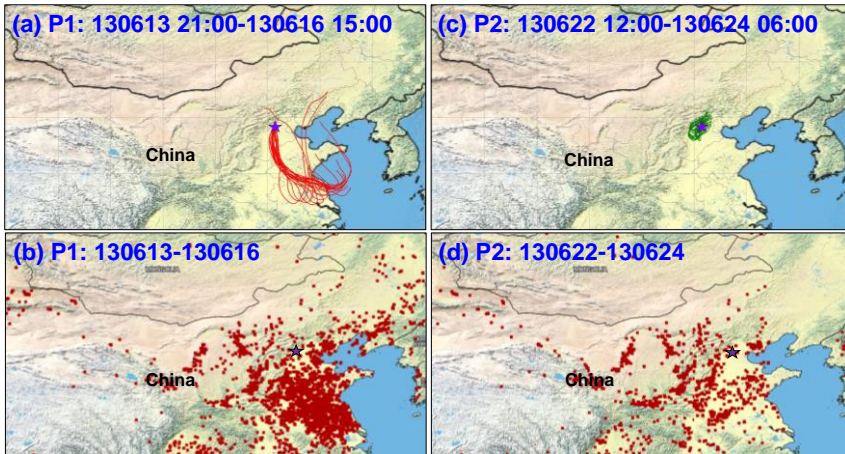
893

894

895

896

897



898

899 Figure 1. Backward trajectories of air masses (a,c) (provided by NOAA HYSPLIT modeling system,
900 <http://ready.arl.noaa.gov/HYSPLIT.php>), and fire spots (b,d) (provided by Fire Information for
901 Resource Management System, FIRMS, <https://firms.modaps.eosdis.nasa.gov/firemap/>), during Period
902 1 (P1) (Jun 13th 21:00-16th 15:00, 2013) and Period 2 (P2) (Jun 22nd 12:00-24th 06:00, 2013). Sampling
903 site represented as purple star.

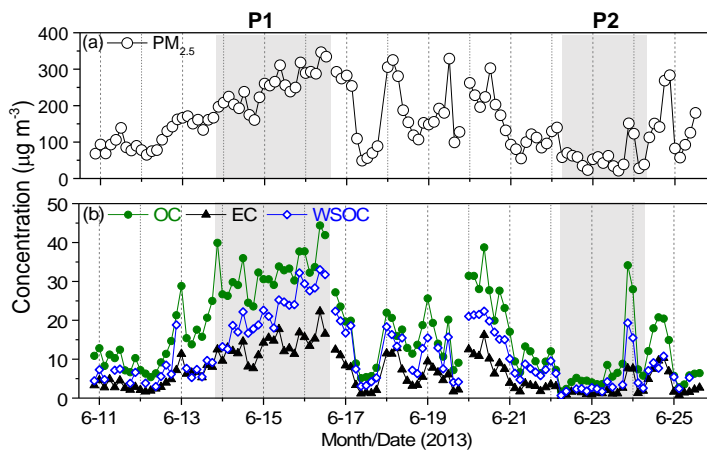
904

905

906

907

908



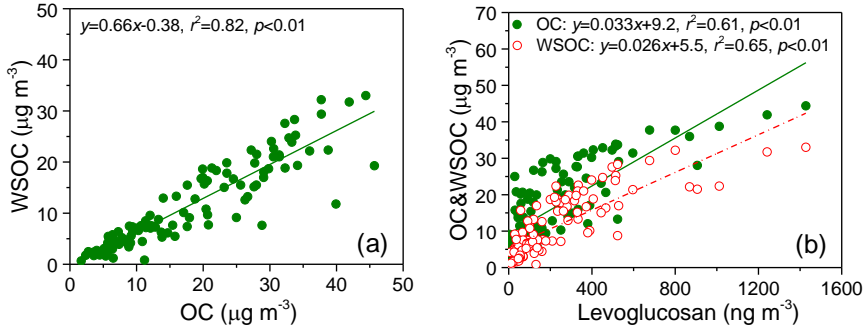
909

910 Figure 2. Temporal variations of PM_{2.5}, OC, EC, and WSOC during the whole sampling period.

911 Shadows denote the two representative periods.

912

913



914

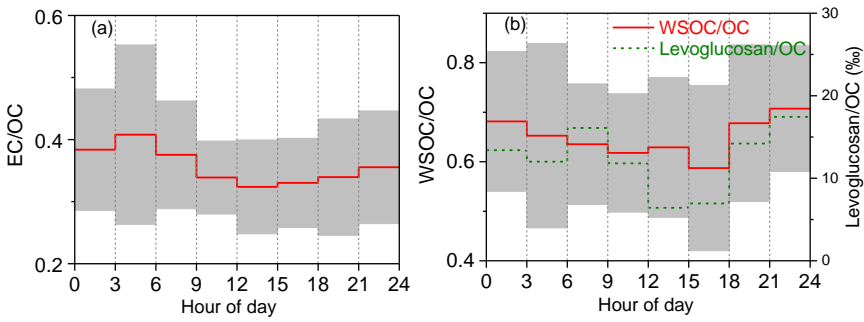
915

916

917

918

Figure 3. Linear correlations of OC with WSOC (a), levoglucosan with OC and WSOC(b).

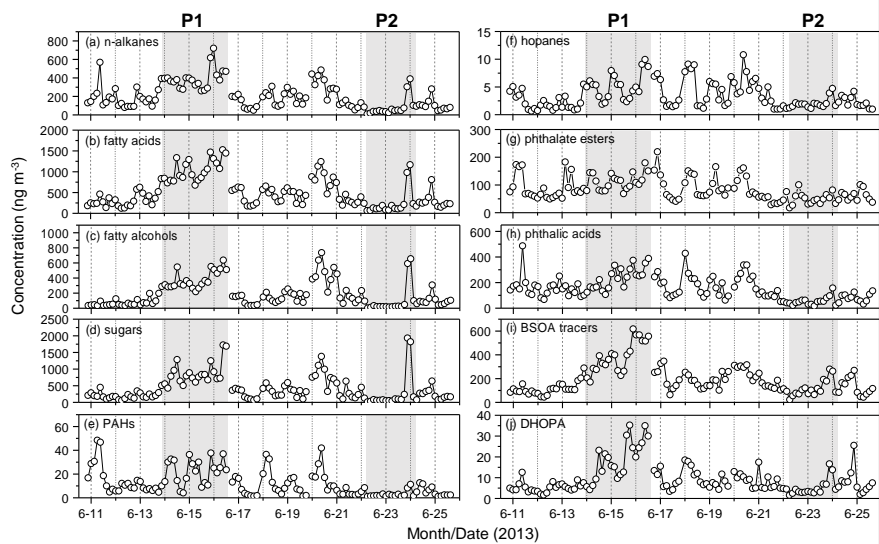


919

920

921

Figure 4. Diurnal variation of OC/EC (a), WSOC/OC and levoglucosan/OC (b).

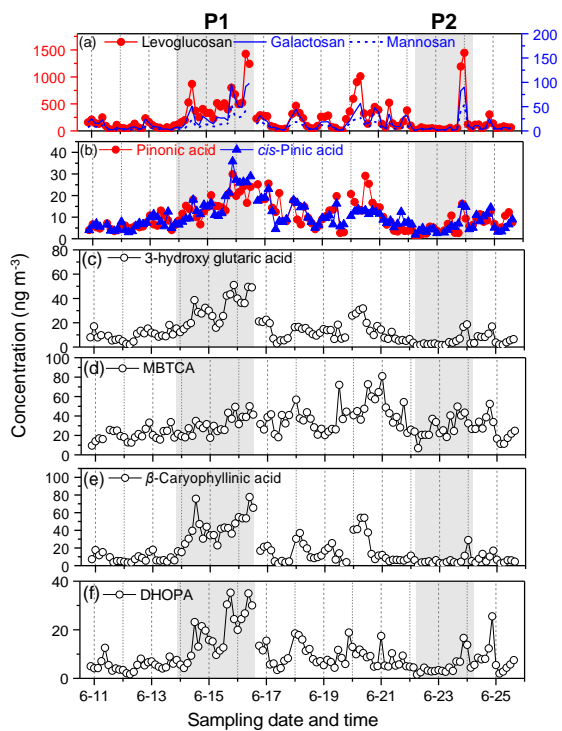


922

923 Figure 5. Temporal variations of ten organic compound classes detected in the summertime PM_{2.5}
 924 samples at the rural site of NCP.

925

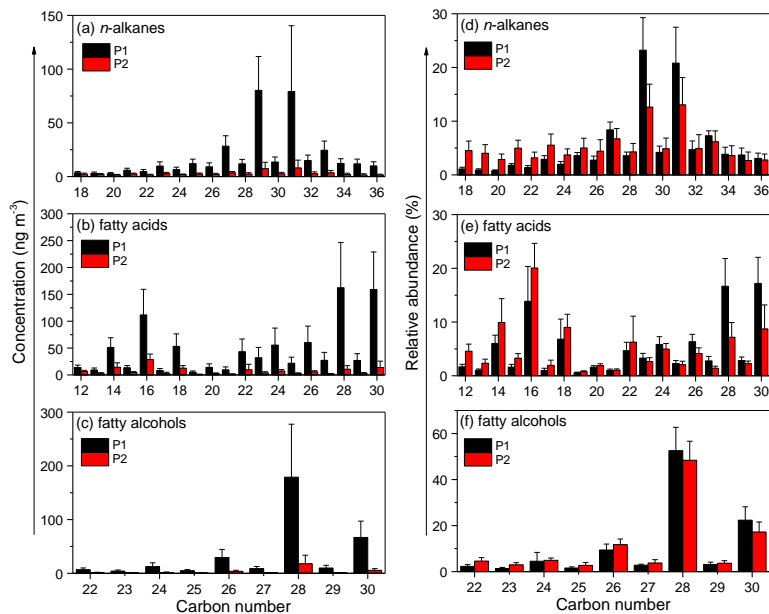
926



927

928 Figure 6. Temporal variations of organic tracers for biomass burning (a), and secondary products
 929 derived from α -/ β -pinene (b-d), β -caryophyllene (e), and toluene (f).

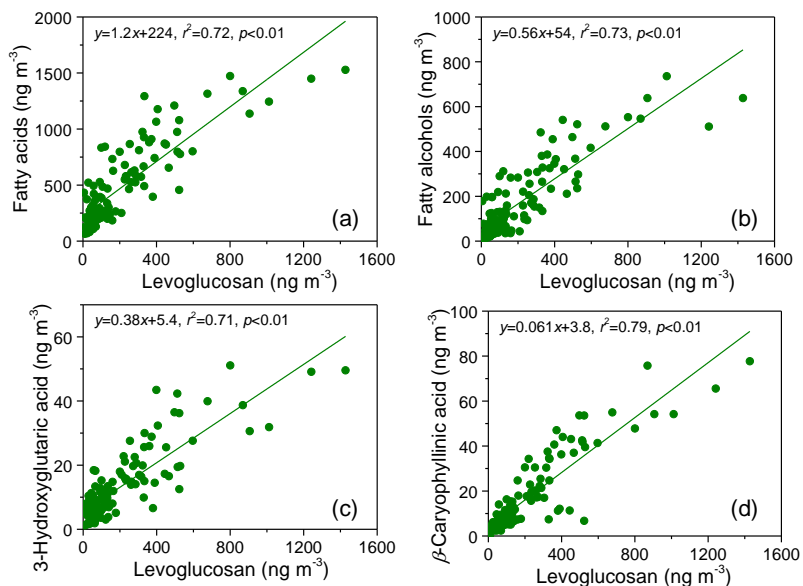
930



931

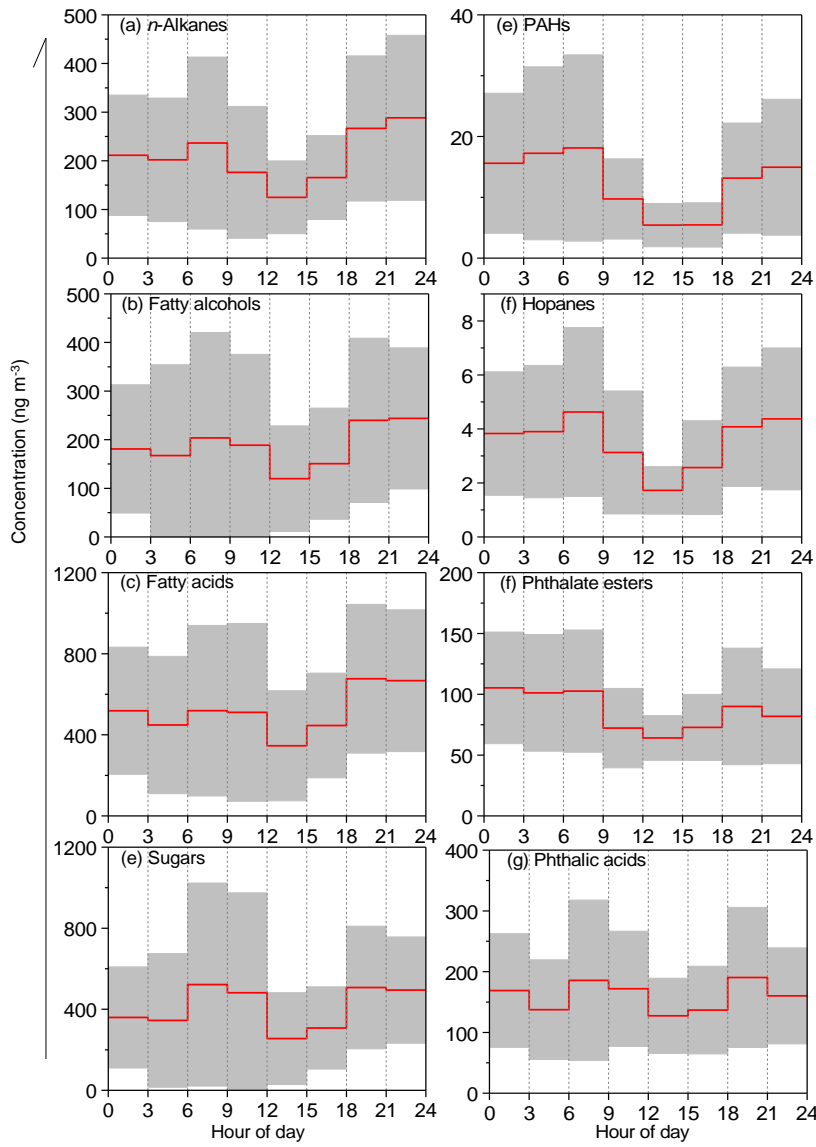
932 Figure 7. Molecular distributions of *n*-alkanes (a and d), fatty acids (b and e), and fatty alcohols (c and
 933 f) in the PM_{2.5} of the rural area.

934



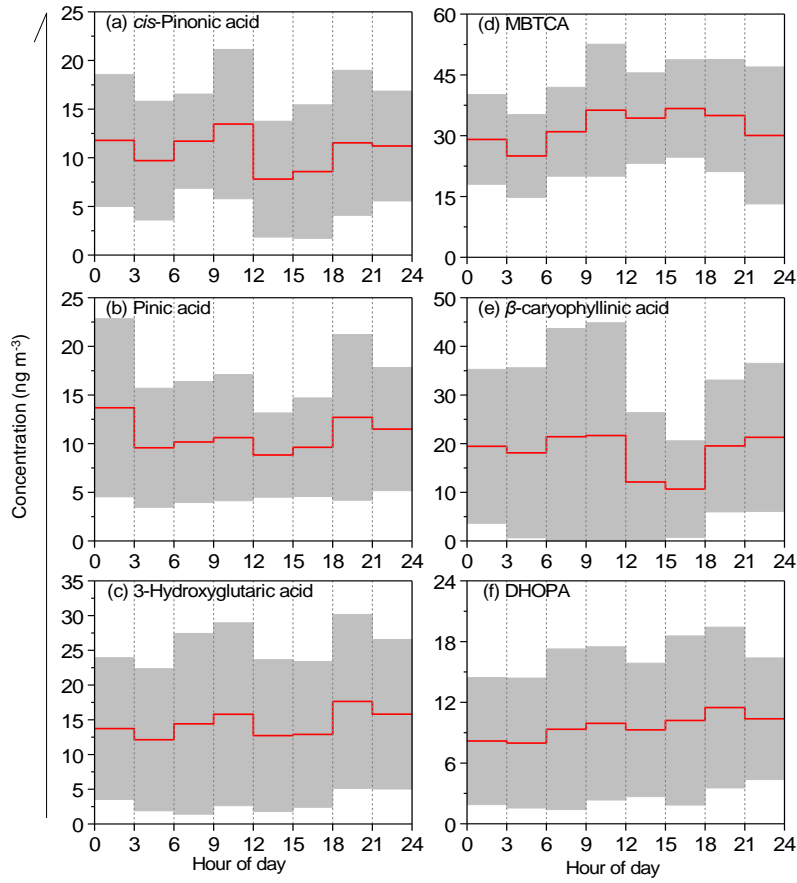
935

936 Figure 8. Linear correlations of fatty acids (a), fatty alcohols (b), 3-hydroxyglutaric acid (c), and β-
 937 caryophyllinic acid (d) with levoglucosan.

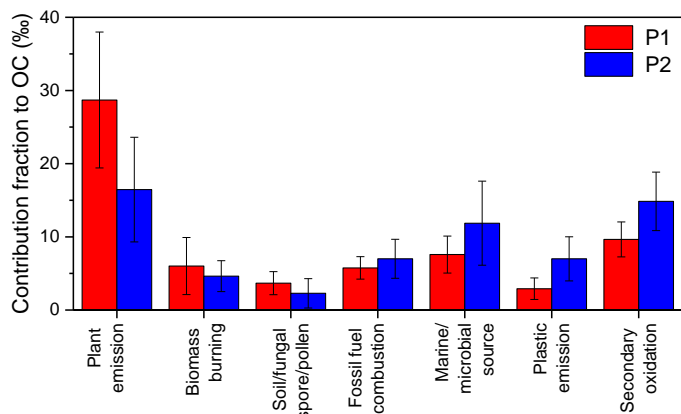


939
 940
 941
 942
 943
 944

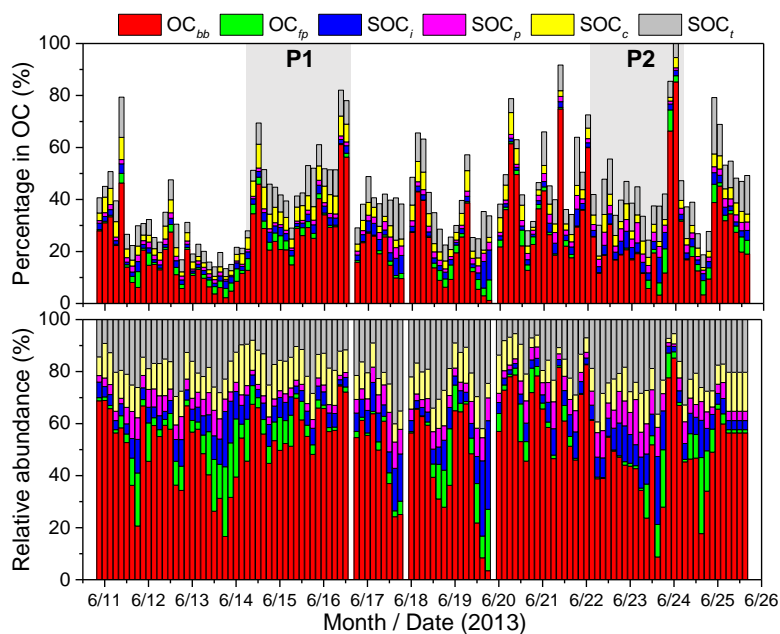
Figure 9. Diurnal variation of the detected organic compound classes.



946
 947 Figure 10. Diurnal variation of the SOA tracers derived from oxidation of α -/ β -pinene (a-d), β -
 948 caryophyllene (e), and toluene (f).
 949
 950

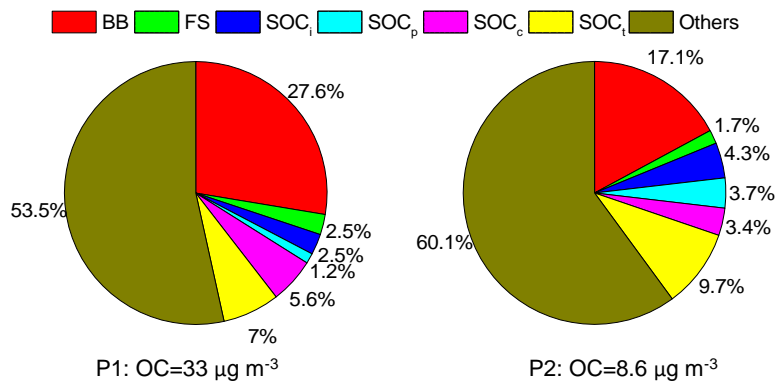


951
 952 Figure 11 A comparison of the average contributions of different sources-derived organics (converted
 953 to carbon content) to OC during P1 and P2.
 954
 955
 956
 957



958
 959 Figure 12. Contributions (above) of primary organic carbon from biomass burning (OC_{bb}) and fungal
 960 spores (OC_{fp}), and secondary organic carbon from isoprene (SOC_i), α - β -pinene (SOC_p), β -
 961 caryophyllene (SOC_c), and toluene (SOC_t) to OC in the time-resolved (3 h) rural aerosols, and their
 962 relative abundances (down). All the contributions were estimated by tracer-based method.
 963

964



965

966 Figure 13. Average contributions of direct emissions from biomass burning (BB) and fungal spores
967 (OC_{sp}), secondary oxidation from isoprene (SOC_i), α - β -pinene (SOC_p), β -caryophyllene (SOC_c), and
968 toluene (SOC_t) to OC in P1 and P2. All the contributions were estimated by tracer-based method.

969

970